Ore Geology Reviews 53 (2013) 357–372

Contents lists available at SciVerse ScienceDirect

Ore Geology Reviews

journal homepage: www.elsevier.com/locate/oregeorev

Strain fabric analysis applied to hydrothermal ore deposits emplaced during changing geodynamical conditions (*Infiernillo* and *Las Picazas*, San Rafael Massif, Argentina)

María S. Japas [a,*], Nora A. Rubinstein [a], Laura E. Kleiman [b]

[a] Instituto de Geociencias Básicas, Aplicadas y Ambientales (IGEBA, UBA-CONICET) Departamento de Ciencias Geológicas, Pabellón II, Ciudad Universitaria, C1428EHA Buenos Aires, Argentina
[b] Comisión Nacional de Energía Atómica, Gerencia de Exploración de Materias Primas. Av. del Libertador 8250, 1419 Buenos Aires, Argentina

ARTICLE INFO

Article history:
Received 14 August 2012
Received in revised form 27 January 2013
Accepted 31 January 2013
Available online 11 February 2013

Keywords:
Tectonic control
Cu–Mo porphyry deposit
Low sulfidation epithermal veins
Permian Choiyoi magmatism

ABSTRACT

Infiernillo and *Las Picazas* are two small hydrothermal ore deposits in the northern San Rafael Massif (Argentina). They are genetically linked to the Permian Choiyoi volcanic province which reflects the transition from a convergent plate margin to an extensional regime: Calc-alkaline Early Permian Lower Choiyoi magmatism was syntectonic with transpressional deformation of the San Rafael Orogeny whereas transitional Late Permian Upper Choiyoi sequences were emplaced under a transtensional regime during the Post-San Rafael extension. *Infiernillo* is a Cu–(Mo) porphyry-type deposit hosted by pyroclastic rocks of the Lower Choiyoi. It consists of a central quartz plug surrounded by a potassic and a phyllic halo, and a set of peripheral polymetallic (Cu–Pb–Zn) veins cropping out close to the alteration zone. The *Las Picazas* deposit consists of a group of low-sulfidation epithermal galena-bearing veins hosted by Early Palaeozoic meta-sediments.

Strain fabric and available 2-D and 3-D kinematic analyses were performed in order to define the relationships between both deposits and the geodynamic scenario. These data reveal that a) porphyry emplacement at *Infiernillo* occurred during the declination of the San Rafael Orogeny, shortly before the change in stress regime, and b) *Las Picazas* low sulfidation epithermal veins were emplaced during the subsequent transtensional Post-San Rafael regime. These results prove that each ore deposit is linked to a different stress regime reflecting the change in geodynamical conditions that prevailed during the emplacement of the Choiyoi volcanism. Thus, strain fabric analysis at both ore deposits allows us to confirm that the tectonic regime is a major factor in controlling the mineralization style of hydrothermal ore deposits.

1. Introduction

Since the Plate Tectonics theory was proposed and accepted during the sixties, identification and understanding of the geodynamical controls on ore deposit formation has been a prolific research field and from that time on, significant insight into the timing and location of ore bodies has been derived from tectonic, geochemical and radiometric data (Jurković and Palinkaš, 2002; Mitchell and Garson, 1981; Pereira and Dixon, 1971; Sillitoe, 1972; von Quadt et al., 2002; among others). Modern research lines have shown that although transitory plate motions alone are insufficient to generate large ore deposits, they emerge as a main trigger for magma-related ore deposits generation (Billa et al., 2004; Blundell et al., 2005; Tosdal and Richards, 2001). In this context, Cu-porphyry, high- and low-sulfidation epithermal ore deposits are key cases to investigate the link between ore deposits styles and specific structural–geodynamical settings, in particular since Sillitoe and Hedenquist (2003) have considered most of the Cu-porphyry provinces and related high sulfidation epithermal deposits as having been generated during compressional (or transpressional) tectonic regimes, and low sulfidation epithermal deposits as related to extensional (rift) settings.

During the Early to Mid Permian (~280–265 Ma), the onset of arc related rocks of the Lower Choiyoi section (Kleiman and Japas, 2009; Llambías et al., 1993) was coeval with the transpressional San Rafael Orogeny. Magmatic composition and the inland expansion of the Lower Choiyoi volcanics, as well as the kinematics of structures reveal a shallowing of the slab at the San Rafael Massif latitude, and the development of a flat slab region south of 36°S (Kleiman and Japas, 2009). The end of subduction, subsequent gravitational collapse of the oceanic plate and concomitant extensional collapse of the orogen resulted in the development of the Upper Choiyoi volcanism by the Mid to Late Permian (~263–251 Ma; Kleiman and Japas, 2009). Intraplate rhyolitic rocks of the Upper Choiyoi section were deformed during transtension (Kleiman and Japas, 2009; Rocha-Campos et al., 2011). Recording the transition from convergence-related to extensional intraplate magmatism, the Permian Choiyoi volcanic province of Argentina and Chile (23°S to 42°S) and its related hydrothermal ore deposits offers an exceptional opportunity to check the hypothetical link between tectonic regime and mineralization style. Both sections of this large magmatic

* Corresponding author at: Departamento de Ciencias Geológicas, Pabellón II, Ciudad Universitaria, C1428EHA Buenos Aires, Argentina. Fax: +54 11 4576 3329.
E-mail addresses: msjapas@gl.fcen.uba.ar (M.S. Japas), nora@gl.fcen.uba.ar (N.A. Rubinstein), kleiman@cae.cnea.gov.ar (L.E. Kleiman).

0169-1368/$ – see front matter © 2013 Elsevier B.V. All rights reserved.
http://dx.doi.org/10.1016/j.oregeorev.2013.01.018

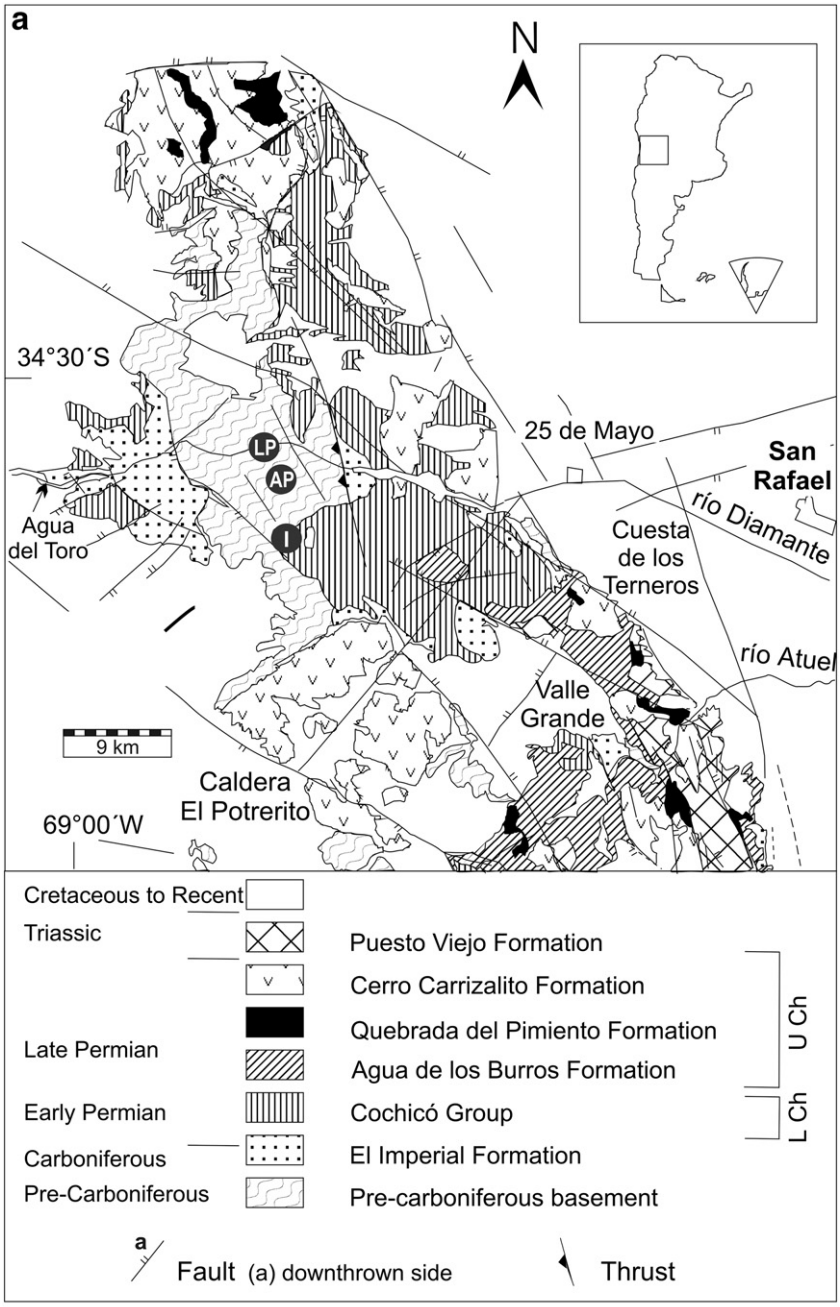
a
N
34°30´S
69°00´W
LP
AP
I
Agua del Toro
25 de Mayo
San Rafael
río Diamante
Cuesta de los Terneros
río Atuel
Valle Grande
Caldera El Potrerito
9 km
Cretaceous to Recent
Triassic
Late Permian
Early Permian
Carboniferous
Pre-Carboniferous
Puesto Viejo Formation
Cerro Carrizalito Formation
Quebrada del Pimiento Formation
Agua de los Burros Formation
Cochicó Group
El Imperial Formation
Pre-carboniferous basement
U Ch
L Ch
Fault (a) downthrown side
Thrust

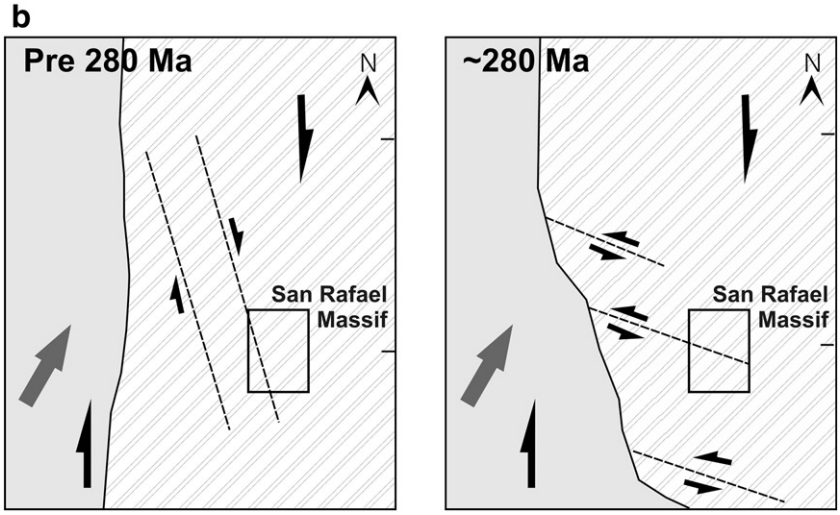
b
Pre 280 Ma
N
San Rafael Massif
~280 Ma
N
San Rafael Massif

episode are well preserved in the San Rafael Massif of western Argentina (Fig. 1a), where the timing of deformation and magmatism is precisely constrained (Kleiman and Japas, 2009).

Based on Pb/Pb model ages and stratigraphic constraints, many hydrothermal ore deposits in the San Rafael Massif were linked to this Permian magmatic episode (Carpio et al., 2001; Rubinstein et al., 2004). A number of Cu–(Mo) porphyry prospects were preliminarily associated with the lower Choiyoi section. Examples include *Infiernillo* (including *Las Picazas* veins), *La Chilca*, *San Pedro* and *Cerro Tres Hermanos* (Delpino et al., 1993; Fuschini, 1968; Gómez and Rubinstein, 2010; Rubinstein et al., 2002a,b, 2012). Related to the upper Choiyoi section there are Mo porphyry prospects, such as *Germán* and *Elsiren* (Carpio et al., 2001; Delpino, 1997) and low-sulfidation epithermal prospects (*El Pantanito* and *Central II*) (Gargiulo et al., 2007; Rubinstein and Gargiulo, 2005; Rubinstein et al., 2001). These different types of mineral systems were linked to the evolution of the Choiyoi magmatic province under a changing tectonic regime (Carpio et al., 2001).

This paper presents strain fabric and kinematic analyses of the *Infiernillo* Cu–(Mo) porphyry deposit and *Las Picazas* low-sulfidation epithermal veins. These deposits were selected for this study because they are linked to the same volcanic cycle and they are located in a geographically restricted area. In spite of their reduced size, low economical potential and present knowledge, *Infiernillo* and *Las Picazas* represent two key cases that demonstrate the geodynamical control on both, low-sulfidation epithermal and porphyry type deposits. Comparisons with published strain fabric data from the San Rafael Massif also allowed us to constrain the timing of both deposits as well as the age of *Infiernillo* porphyry emplacement. Thus, strain fabric analysis could be a complementary low-cost tool in ore deposit research and exploration.

2. Methods

This paper is focused on strain fabric analysis at the *Infiernillo* and at *Las Picazas* ore deposits; therefore a conventional analysis of the whole structure was not performed in this study.

"Fabric" is regarded as the "complete spatial and geometrical configuration of all those components (fabric elements) that make up a rock" (Hobbs et al., 1976). In order to be considered as fabric elements, structures must be penetrative and repeatedly distributed throughout the rock (see Hobbs et al., 1976; Passchier and Trouw, 1996). Because the fabric elements analyzed in this paper resulted from deformation, the studied fabric will be considered here as "Strain Fabric" (see Chardon et al., 2002; Lenauer and Riller, 2012; Taylor, 2009 p. 76). To avoid some of the ambiguity associated with the scale-dependant elements to be considered in a strain fabric analysis, we point out that this study was carried out at the outcrop scale. With this in mind, the fabric elements evaluated are: a) shape of strained geological elements, such as elliptical alteration haloes, distribution of geochemical anomalies and fracture patterns and b) planar structures such as brittle–ductile shear zones (following Ramsay and Huber, 1987) and fractures (tensional, shear extensional; Hancock, 1985) (Fig. 2a); microfabric elements (grain attributes) were not considered in the present analysis. Brittle–ductile, transpressional and transtensional shear zones (following Dewey et al., 1998; Sanderson and Marchini, 1984; Tikoff and Greene, 1997) were defined on the basis of a) geometrical relationships between fabric elements and b) kinematic indicators. Kinematics was established by the offset of structures, presence of releasing/restraining bends, progressive evolution of minor structures (e.g.: folding of earlier veins) as well as by distribution of *en-échèlon* gashes, tensional fractures, rough cleavage and/or Riedel structures. Tensional fractures were recognized based on the absence of slip whereas shear extensional

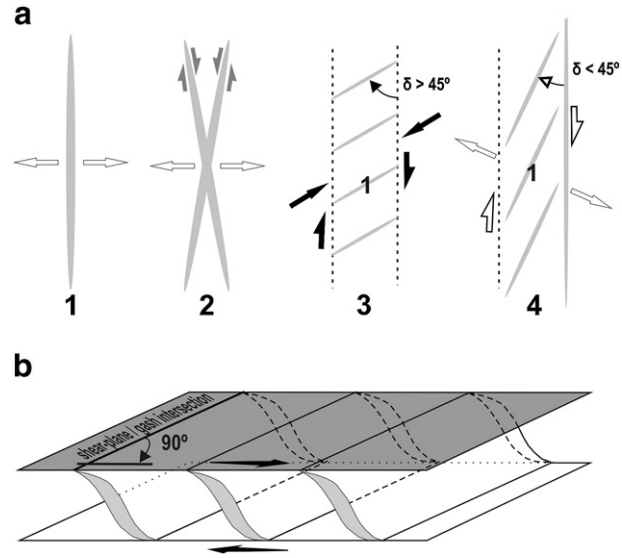

Fig. 2. Kinematic indicators. a. Different types of structures that were considered in this contribution. 1: Tensional veins and fractures; 2: Shear extensional veins and fractures; 3: Brittle–ductile transpressional shear zones with linked tensional fractures; 4: Brittle–ductile transtensional shear zones displaying tensional fractures. It must be noted that the presence of straight/planar tensional fl1 veins instead of more sigmoidal ones does not necessarily imply a pure shear regime, because their presence could also be explained during simple shearing by differences in inter-vein distances (that would trigger or not bridge deformation; Bons et al., 2012; Peacock, 1991; Olson and Pollard, 1991; Smith, 1996), and/or rheological properties of rocks (mechanical stratigraphy, Bons et al., 2012; different rock strength/stress ratio, Olson and Pollard, 1991; affected rock thickness, Smith, 1996). Transpression and transtension refer to strike–slip deformations that deviate from simple shear because of a component of, respectively, shortening (3) or extension (4). Notice that this component of shortening and extension imposes tensional fractures at respectively higher (>45°) and lower (<45°) angles to the zone boundaries than in simple shear strike slip (45°). b. Calculation of direction and sense of movement of brittle–ductile shear zones based on minor structures (see explanation in Section 2).

fractures and their kinematics were identified by the presence of dilatational jogs and offset of other fabric elements. Timing of minor structures was defined by cross-cutting, overprinting and reactivation relationships.

The strain fabrics of some key areas at the *Infiernillo* and at *Las Picazas* deposits were analyzed. Orientation, relative motions and geometrical and cross-cutting relationships of strain fabric elements as well as shape-preferred orientation of alteration haloes were measured and linked with the alteration zones. The results of these analyses were compared with previous strain fabric data from other Permian rocks at the San Rafael Massif (Kleiman and Japas, 2009, and references therein).

The 3-D kinematic analysis allowed us to define the kinematic axes of the deformational regime, which were compared with previous published data obtained by Kleiman and Japas (2009). Where possible, 3-D kinematic measurements on minor structures related to mineralized veins were performed (e.g.: *en-échèlon* gashes, Riedel structures, etc.). Instead of traditional kinematic measurements of striae on fault surfaces (which commonly record only the last relative movement) we used these minor structures as they preserve the kinematic history even when they are overprinted by later events. In this way, Cortés et al. (2009) confirmed a unique kinematic result regardless the kinematic indicator (striae and tensional fractures) used. In addition, Japas et al. (2010) and Sruoga et al. (2010) demonstrated that using minor structures as 3-D kinematic indicators, it is possible to discriminate the distinct populations of different deformational stages in a comparable manner as Lisle and Vandycke (1996) have done. As real "kinematic memory" of rocks, these minor structures permitted the identification

Fig. 1. a. Location of the study area, and geological map from northern San Rafael Massif (after Kleiman, 1999; Kleiman and Japas, 2009). I: *Infiernillo*, LP: *Las Picazas*, AP: *Agua de Pablito*. LCh: Lower Choiyoi; UCh: Upper Choiyoi. b. Deformation of the SW margin of Gondwana (29°–36°S segment) during the Early Permian (after Kleiman and Japas, 2009). Left: first stage of the San Rafael Orogeny (SRO1); right: second stage of the San Rafael Orogeny (SRO2).

Table 1
Stratigraphy of the San Rafael Massif.
After Carpio et al., 2001 and Kleiman and Japas, 2009.

Time		Units			Rock sequence	Cycle	Tectonic events
Late Cretaceous to Quaternary					Back-arc magmatism Back-arc continental deposits	Andean	Andean Orogeny
Triassic		Puesto Viejo Fm ~241-235 Ma			Synrift-continental successions Alkaline and bimodal magmatism	Gondwanian	Rifting
Permian	Late	Choiyoi	Upper Choiyoi	Cerro Carrizalito Fm ~252 Ma Quebrada del Pimiento Fm Agua de los Burros Fm ~265 Ma	Volcanic sequence (post-orogenic silicic magmatism)		Post-San Rafael Extension (transtension)
	Early		Lower Choiyoi	Cochicó Gr ~281 Ma	Volcano-sedimentary sequence (arc magmatism)		San Rafael Orogeny (transpression)
Carboniferous		El Imperial Fm			Foreland deposits		Chanic Phase
Devonian		La Horqueta / Río Seco de los Castaños Fm			Passive margin deposits?	Famatinian	Ocloyic Phase
Silurian							
Ordovician		Pavón Fm Lindero Fm Ponón Trehué Fm			Carbonate platform sequences Igneous rocks (ultramafic belt)		
Proterozoic		Cerro La Ventana Fm			Metamorphic and igneous rocks	Grenvillian	

of direction and sense of movement: Direction of movement is defined by the perpendicular to the intersection of the gash/R structure with the fault or shear zone whereas its sense is indicated by the asymmetry of the gash/R structure (Fig. 2b; Japas et al., 2008; see also Becker and Gross, 1999).

3. Geological setting

The San Rafael Massif is located in the central part of southern Mendoza, Argentina (Fig. 1a). Precambrian outcrops are scarce in the area. From the Ordovician to the Early Permian, sediments were deposited and successively deformed during the Mid-Late Ordovician, the Late Devonian and the Early Permian (Table 1). The Early Permian orogeny marked the end of the sedimentation and the beginning of the Choiyoi magmatic cycle which represents a transition between a magmatic arc to a rift tectonic setting (Kleiman and Japas, 2009; Kleiman and Salvarredi, 2001). From the Late Cretaceous to the Pleistocene, the geological record shows a sequence of continental sedimentary rocks and volcanic back-arc products that were deformed by the different phases of the Andean Orogeny (Narciso et al., 2007; Sepúlveda et al., 2007a,b).

3.1. Permian Gondwana magmatism and deformation in the San Rafael Massif

Emplaced in a magmatic arc setting, the Early to Middle Permian Cochicó Group (lower Choiyoi section, Fig. 1a and Table 1) is represented by andesites and dacitic to low-silica rhyolitic ignimbrites with associated sedimentary rocks (Kleiman, 1993, 1999; Kleiman and Japas, 2002). The onset of the Lower Choiyoi was coeval with the transpression of the San Rafael Orogeny (SRO, Kleiman and Japas, 2009).

The upper Choiyoi section (Middle to Late Permian, Fig. 1a and Table 1) includes the Agua de los Burros, the Quebrada del Pimiento and the Cerro Carrizalito Formations (González Díaz, 1973). These successions comprise rhyolitic ignimbrites and lava flows, dacitic to rhyolitic subvolcanics, andesitic dikes and alkalic basaltic andesites (Kleiman, 1999, 2002). Although Agua de los Burros Formation volcanics are geochemically more akin with the upper Choiyoi section, these rocks are affected by the transpressional deformation of the San Rafael Orogeny. The Quebrada del Pimiento and Cerro Carrizalito Formations were emplaced under the transtensional deformation of the Post-San Rafael event (PSR, Kleiman and Japas, 2009).

Permian transpressional and transtensional deformation show a high degree of partitioning of motions at the regional scale that could have been conditioned by WNW to ENE and NW Precambrian anisotropies, and the NNW Early Paleozoic structural grain (Kleiman and Japas, 2009). Based on relationships between *en-échèlon* folds, faults and brittle–ductile shear zones, three different domains were defined (North, Central and South, Japas and Kleiman, 2004; Japas and Tomezzoli, 2001; Kleiman and Japas, 2009) (Fig. 3a and b). During the San Rafael Orogeny, the North domain was deformed by WNW-trending sinistral transpression, the South domain by NS dextral transpression and the Central domain by dextral and sinistral transpression overprinted by NW thrusting (Kleiman and Japas, 2009; Fig. 3a). Minor structures reveal the superposition of two stages of deformation within the San Rafael orogeny (Kleiman and Japas, 2009): a first main stage of N–NNW dextral, pure-shear-dominated transpression (SRO1; $\alpha \sim 30°$) was followed by a second stage of WNW sinistral, pure-shear-dominated transpression (SRO2; $\alpha \sim 70°$) that was synchronous with the emplacement of the Cochicó Group (Kleiman and Japas, 2009). This second stage of deformation is more evident in the North Domain. The angular relationship between the WNW regional shear zone and the NNE shortening direction for the second stage of the San Rafael Orogeny ($\alpha \sim 80°$) resulted in transpression, a situation that is comparable with the Argentine Precordillera modern analog (28°S–38°S, Central Andes, see Siame et al., 2005). The low angle of partitioning recognized for the San Rafael Orogeny (SRO2; Kleiman and Japas, 2009) resulted in a low degree of misfit between the plate motion and the minimum infinitesimal stretching axis (see Fossen and Tikoff, 1998). Considering the curvature of the margin south of 31°S from ~NS in the north to NW in the south (Fig. 1b), and the NNE convergence direction by the Early Permian (Kleiman and Japas, 2009), the second stage of the San Rafael Orogeny at San Rafael should have been linked to a "transpressional" restraining bend (see Mann, 2007).

During the Late Permian Post-San Rafael extension, tectonic reversion occurred, since its direction of maximum extension is coincident with the maximum compression direction of the previous San Rafael

orogeny (Kleiman and Japas, 2009; Fig. 3a and b). Because North, South and Central domains remained active, then Post-San Rafael extension resulted in WNW dextral transtension (North), NNW sinistral transtension (South) and NW-trending tensional structures (Central) (Japas and Kleiman, 2004; Kleiman and Japas, 2009; Fig. 3b).

Since they are located within the Northern Domain of the San Rafael Massif (Fig. 1a), the *Infiernillo* and *Las Picazas* areas should have undergone NNW dextral transpression (SRO1), WNW sinistral transpression (SRO2) during the Early Permian San Rafael Orogeny, and WNW dextral transtension during the Late Permian Post-San Rafael extension.

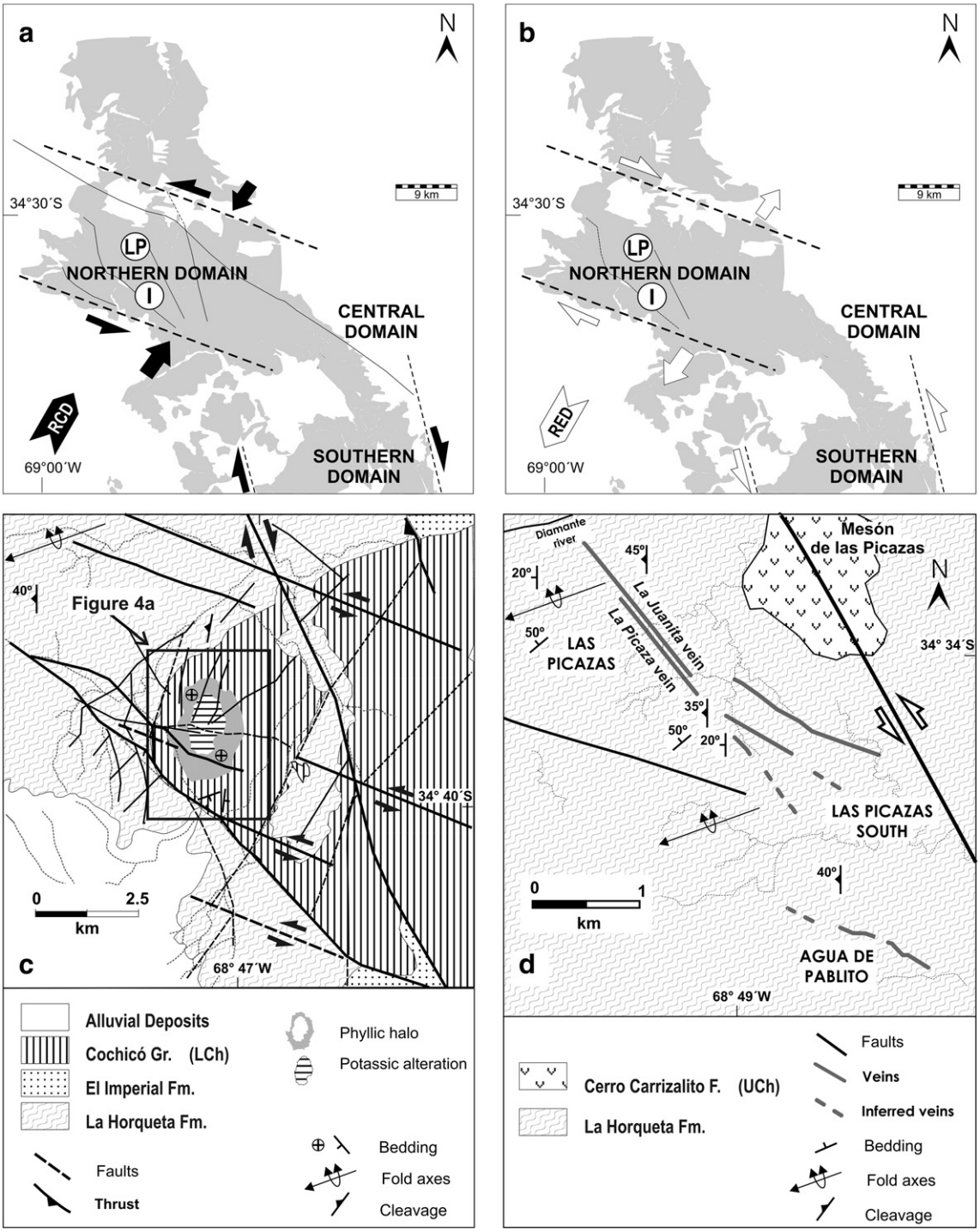

Fig. 3. *Infiernillo* and *Las Picazas* deposits in the geological context. a,b. Structural domains and their kinematic (based on Kleiman and Japas, 2009). a. San Rafael Orogeny and main contractional structures in the study area (Northern Domain); RCD: regional contractional direction. b. Post-San Rafael extension and main extensional structures in the study area. Some of these structures are reactivated structures; RED: regional extensional direction. I: *Infiernillo*; LP: *Las Picazas* (modified from Kleiman and Japas, 2009). c. *Infiernillo* geological map (modified from Gómez, 2008). Notice that *Infiernillo* deposit is localized where two sets of faults (WNW and NNW) cross-cut. NNW-trending faults show dextral transpressional motions (as shown) but also sinistral transtensional reactivations (Kleiman and Japas, 2009). LCh: Lower Choiyoi. d. *Las Picazas* geological map showing the two measured localities (*Las Picazas* and *Las Picazas S*). UCh: Upper Choiyoi.

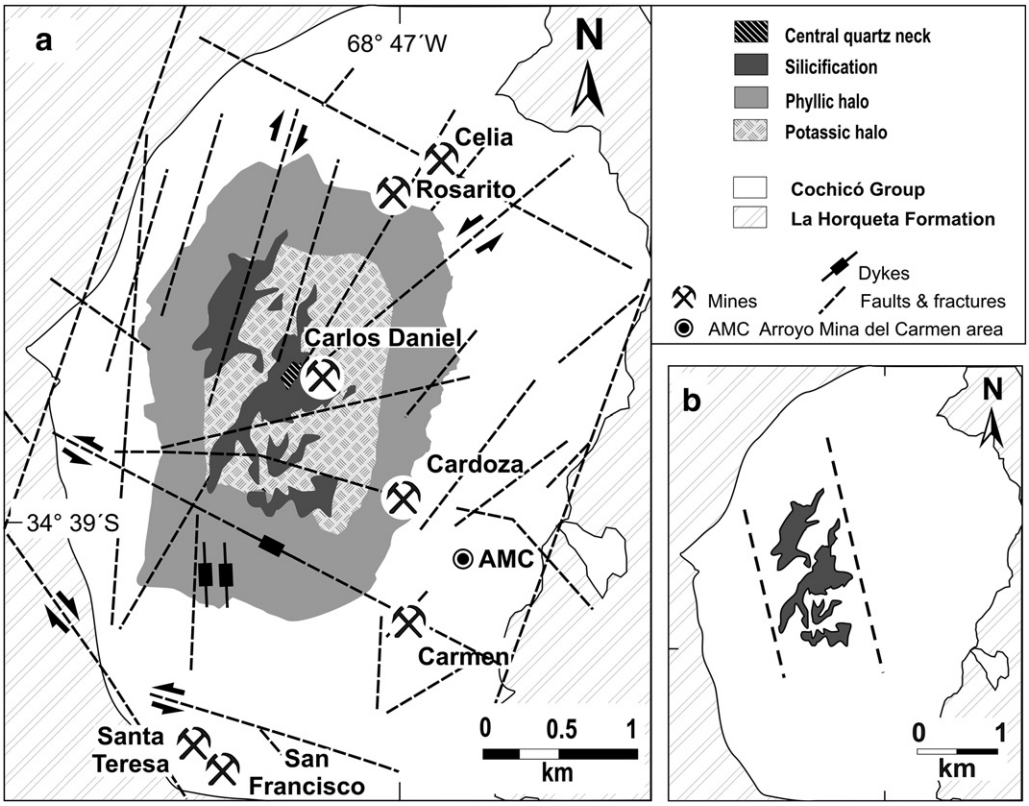

Fig. 4. *Infiernillo* alteration zone. a. *Infiernillo* alteration area and mines (adapted from Fuschini, 1968 and Gómez and Rubinstein, 2010). Potassic and phyllic alteration are shown. 2-D kinematic indicators indicate fault displacement as shown but also later reactivation coherent with motions revealed by displacement of the phyllic halo. Cu and Mo are distributed around the central quartz plug in those areas showing weak silicification. b. The three main in-veinlet silicified zones shown in (a) are aligned following a NNW direction suggesting they would be controlled by a brittle–ductile shear zone (dashed lines). NNW-striking Upper Choiyoi andesitic dykes were emplaced following this structure.

4. Mineral deposits

The *Infiernillo* and *Las Picazas* deposits share a common hydrothermal origin linked to the Choiyoi magmatic cycle. *Infiernillo* (34° 38′ 22″ S, 68° 47′51″ W) is a low grade Cu–Mo porphyry prospect (Di Tommaso and Rubinstein, 2007; Fuschini, 1968), hosted by the Cochicó Group (Fig. 3c). *Las Picazas* (34° 33′57″ S, 68° 49′34″ W, Fig. 3d) consists of a group of galena-bearing veins hosted by Early Palaeozoic schists (Fuschini, 1968) preliminarily interpreted as the roots of a low sulfidation epithermal system (Rubinstein et al., 2008).

4.1. Infiernillo ore deposit

Exploration at the *Infiernillo* prospect started in the early 1960s and finished in 1967 (Fuschini, 1968). This prospect is hosted by rhyolitic tuffs from the lower section of the Choiyoi (Fig. 3c). The alteration zone has an oval shape with a NNE–SSW trend (Di Tommaso and Rubinstein, 2007; Fuschini, 1968) (Figs. 3c and 4a). Airborne magnetometric data (Johanis, 2003) show a positive anomaly approximately coincident with the potassic zone, surrounded by a relatively low magnetic intensity halo suggesting magnetite destruction, typical of the phyllic zone in porphyry deposits (Clark, 1999).

According to Fuschini (1968) the deposit is deformed by heterogeneously distributed faults arranged in a radial pattern; faults tend to be more conspicuous to the east and to the south, and control the mineralization. The core consists of a NNE oriented elliptical quartz plug (*Carlos Daniel* mine area, Fig. 4a) which includes stockwork and silicified host rock fragments. Two silicification stages were recognized in the quartz cement (Korzeniewski et al., 2008): the first consists of quartz crystal aggregates and the second is made up of quartz with textures typical of epithermal deposits. The quartz plug is surrounded by a quartz stockwork with pyrite and hematite. High temperature (>350°) and high salinity (30–55 wt.% NaCl eq.) inclusions were recognized in the stockwork veins (Korzeniewski et al., 2008). Surrounding the quartz plug there is a potassic alteration zone (Fig. 4a) which consists of pervasive K-feldspathization, silicification and minor biotitization.

Outwards of the potassic alteration zone there is a phyllic halo (Fig. 4a) which is extensively oxidized and consists of pervasive and veinlet-type silicification and pervasive sericitization. Abundant pyrite occurs both disseminated and in veinlets. A late carbonatization process, which occurs as veins and to a lesser degree pervasively, overprints both the potassic and phyllic alteration (Di Tommaso and Rubinstein, 2007).

The ore minerals occur disseminated and in quartz veinlets (Gómez and Rubinstein, 2010). In the potassic alteration zone the paragenetic sequence is: bornite, chalcopyrite–molybdenite, pyrite (galena–sphalerite), chalcocite–covellite. In the phyllic zone the paragenetic sequence is: chalcopyrite, molybdenite and pyrite. Surface geochemical analyses reveal nearly coincident anomalies of Cu and Mo located at the inner border of the phyllic halo (Di Tommaso and Rubinstein, 2007; Fuschini, 1968) (Fig. 4a).

Small polymetallic veins with lead–zinc–silver mineralization crop out within or surrounding the phyllic halo (*Cardoza*, *San Francisco*, *Santa Teresa*, *Carmen*, *Rosarito* and *Celia* veins, Fig. 4a, Table 2). Low temperature (335°–210 °C) and low salinity (20–0.5 wt.% NaCl eq.) inclusions were recognized in these veins and also in the stockwork surrounding the quartz plug (Korzeniewski et al., 2008).

The ore assemblage of the polymetallic veins consists of pyrite, galena and sphalerite and minor arsenopyrite, chalcopyrite, magnetite, tetrahedrite and electrum in a quartz gangue. The host rocks show intense and mainly pervasive silicification and sericitization close to the contact with the veins (Gómez and Rubinstein, 2010).

Table 2
Location and main characteristics of the polymetallic veins of the district (from Fuschini, 1968; Gómez and Rubinstein, 2008; Japas and Rubinstein, 2006). Ga: galena; py: pyrite; sph: sphalerite; asp: arsenopyrite; cpy: chalcopyrite, ag-td: ag-tetrahedrite; el: electrum. Silic: Silicification; ser: sericitization.

Mine	Ore minerals	Gangue	Wall rock alteration
Cardoza	Ga, py	Quartz	Silic — ser
San Francisco	Ga, py	Quartz	Silic — ser
Santa Teresa	Ga, py, asp, sph, cpy, (el)	Quartz	Silic — ser
Carmen	Ga, py, sph, asp	Quartz	Silic
Rosarito	Ga, sph, ag-td, cpy, mg	Quartz, carbonate	Silic — ser Carbonatization
Celia	Gal, asp	Quartz	Silic — ser
Las Picazas	Py, ga, asp, sph, (cpy desease), (cv)	Quartz	Silic — ser Carbonatization
Agua de Pablito	Py, ga, chpy, ac, (cv)	Quartz, opal, (fluorite)	Silic — ser

4.2. Las Picazas mine

Las Picazas mine comprises a set of NW-trending galena-bearing veins (Fuschini, 1968), hosted by the La Horqueta Formation (Fig. 3d). The two main veins are named *La Juanita* and *La Picaza*. This mine was sporadically mined from the end of the 19th century until the early 1930s (Carpio, 1999).

The ore assemblage is composed of galena, pyrite, arsenopyrite and sphalerite in a drusy quartz gangue (Table 2). Two quartz stages were recognized: the first is spatially associated with the mineralization and is composed of fine-grained quartz aggregates and the second has textures typical of epithermal ore deposits (Rubinstein et al., 2008). Close to the contact with the veins, the host rocks show intense pervasive sericitization and in-vein silicification.

About 3 km to the SE (34° 35′17″ S, 68° 48′08″ W) the *Agua del Pablito* veins crop out (Carpio et al., 2001) (Fig. 3d, Table 2). The ore paragenesis consists of galena with minor pyrite and pyrrothite and scarce chalcopyrite and acantite. The gangue has drusy texture and consists of opal and zoned quartz. Fluid inclusions studies reveal temperatures of up to 200 °C (Korzeniewski, personal communication). Close to the contact with the veins the schists show intense pervasive sericitization and in-vein and pervasive silicification. Because of their localization and similar trend and mineralogy to those of *Las Picazas*, *Agua de Pablito* veins are preliminary linked with the *Las Picazas* ore deposit.

5. Strain fabric analysis

Selected study areas at *Infiernillo* include the *Carlos Daniel* (central quartz plug and surrounding potassic halo), *Cardoza* (phyllic halo), and *Santa Teresa–San Francisco* and *Carmen* (close to the external border of the phyllic halo) areas (Fig. 4a). The strain fabric analysis at *Las Picazas* was carried out for the *Las Picazas* and *Las Picazas S* regions (W and SW from cerro Mesón de las Picazas, respectively) (Fig. 3d). Additionally, structural data from *Agua del Pablito* veins from Carpio et al. (2001) were considered for this analysis.

5.1. Infiernillo ore deposit

At the *Infiernillo* deposit scale, the hydrothermal alteration area presents a well defined elliptical shape with its maximum axis trending NNE (Fig. 4a).

Some alteration zones such as veins and silicified zones are asymmetrically distributed, and fractures also show an asymmetric pattern (Fig. 4a). Tensional to shear extensional mineralized veins are only present around the eastern border of the *Infiernillo* alteration area (Fig. 4a). Within the potassic halo, three in-veinlets silicified zones show elliptical shapes with a general NNE trend, and are aligned in a NNW direction (Figs. 4a and b). Fractures show two different fabrics. A nearly-radial array of barren sub-vertical fractures striking NNE (010°–040°), ENE (080°) and WNW (120°) affects the core of the alteration zone particularly at the eastern half of *Infiernillo*. On the other hand, a barren NNE fracture set deforms the western alteration zone (Fig. 4a). This overall non-symmetric pattern is coincident with the magnetic minimums reported by Johanis (2003).

Minor structures are heterogeneously distributed around *Infiernillo* and define specific structural grains at each alteration zone. Except where indicated, structures are nearly vertical (Fig. 5).

At the central quartz plug (*Carlos Daniel mine*, Fig. 5ai and bi), a strong NNE (010°–030°/80°E) joint fabric is present. Silicified breccias striking ENE (080°) are the most conspicuous feature in this area. They are dextrally displaced by late WNW (110°) brittle–ductile shear zones.

Within the potassic halo, and near the quartz plug, there is a stockwork structure composed of three sets of thin, sub-vertical quartz–hematite veinlets striking NE (040°), ENE (080°) and WNW (120°) (Figs. 5ai, bi and 6a). These sets show the same trends as the nearly-radial fracture system previously described. Towards the outer border of the potassic halo, NNE (020°–040°) shear extensional and NNE (030°) tensional fractures are predominant (Fig. 5ai). Brittle–ductile transpressional shear zones are frequent in this sector, with two main sets: WNW (110°) sinistral and NNW (150°) dextral (the latter is not represented in Fig. 5a because of the unknown dip angles). Some WNW sets display a rough cleavage or brecciation. Commonly they show dextral transtensional reactivation (Figs. 5a, 6b and c). The NNW set, instead, records sinistral transtensional reactivation.

Within the phyllic halo a strong planar fabric defined by fractures and brittle–ductile shear zones developed in the host rocks at the *Cardoza* mine (Fig. 5aii and bii). This structure striking NNE (025°–030°) is parallel to the local phyllic alteration fringe. 2-D kinematic indicators reveal shear extensional fractures striking close to Az. 020° (normal-dextral components of motions), and to ~Az. 030° (normal-sinistral movements). The ~NNE dextral shear extensional set is predominant (Fig. 5a). Mineralized veins strike at 025°/80°W (*Cardoza Oeste* and *Cardoza Este* veins). Late barren calcite veins are widespread all over this area displaying a typical transtensional pattern (Figs. 5bii and 6d). They comprise tensional fractures (NW, 130°) linked to reactivated transtensional structures (WNW, 110°–125°, dextral, and scarce NNW, 150°, sinistral; Fig. 5aii and bii). Also, ENE-striking, dextral transtensional brittle–ductile shear zones are present.

Close to the outer border of the phyllic halo, some small polymetallic veins crop out (*Santa Teresa*, *San Francisco*, *Carmen*, *Celia* and *Rosarito* veins; Fig. 4a). They constitute fillings of NNE striking (020°–045°) tensional and shear extensional fractures (Figs. 5aiii–iv, biii and 6e). Vein strikes at the *Celia* and *Rosarito* mines are referred to Fuschini (1968) and Gómez and Rubinstein (2008) as NNE (20° subvertical and 5°–10° to 30°/70° W, respectively). Transpressional zones are also frequent showing both sinistral (WNW, 110°) and dextral (NNW, 150°) motions (Fig. 5aiii–iv). Transtensional structures filled with late hydrothermal calcite show similar patterns to those observed at the *Cardoza* mine area (Fig. 5aiii–iv and biii). This transtensional strain fabric is best defined at the Arroyo del Carmen area (WNW, 110°–125°, dextral and NNW, 150°, sinistral; Figs. 4a, 5av and bv), confirming that deformation is strongly heterogeneous.

In summary, two strain fabrics (fl1 and fl2) were recognized at *Infiernillo* based on cross-cutting, re-shearing and overprinting relationships (that also allowed us to recognize their timing), vein infill composition, orientation of tensional shear extensional fractures as well as nature and attitude of brittle–ductile shear zones (Fig. 5a and b). NNE tensional to shear extensional fractures, and WNW and NNW transpressional structures (fl1) overprinted and/or reactivated by NW tensional, and WNW and NNW transtensional structures (fl2). The earlier fabric shows a structural zoning defined by a typical array for each alteration zone whereas the later is homogeneously distributed.

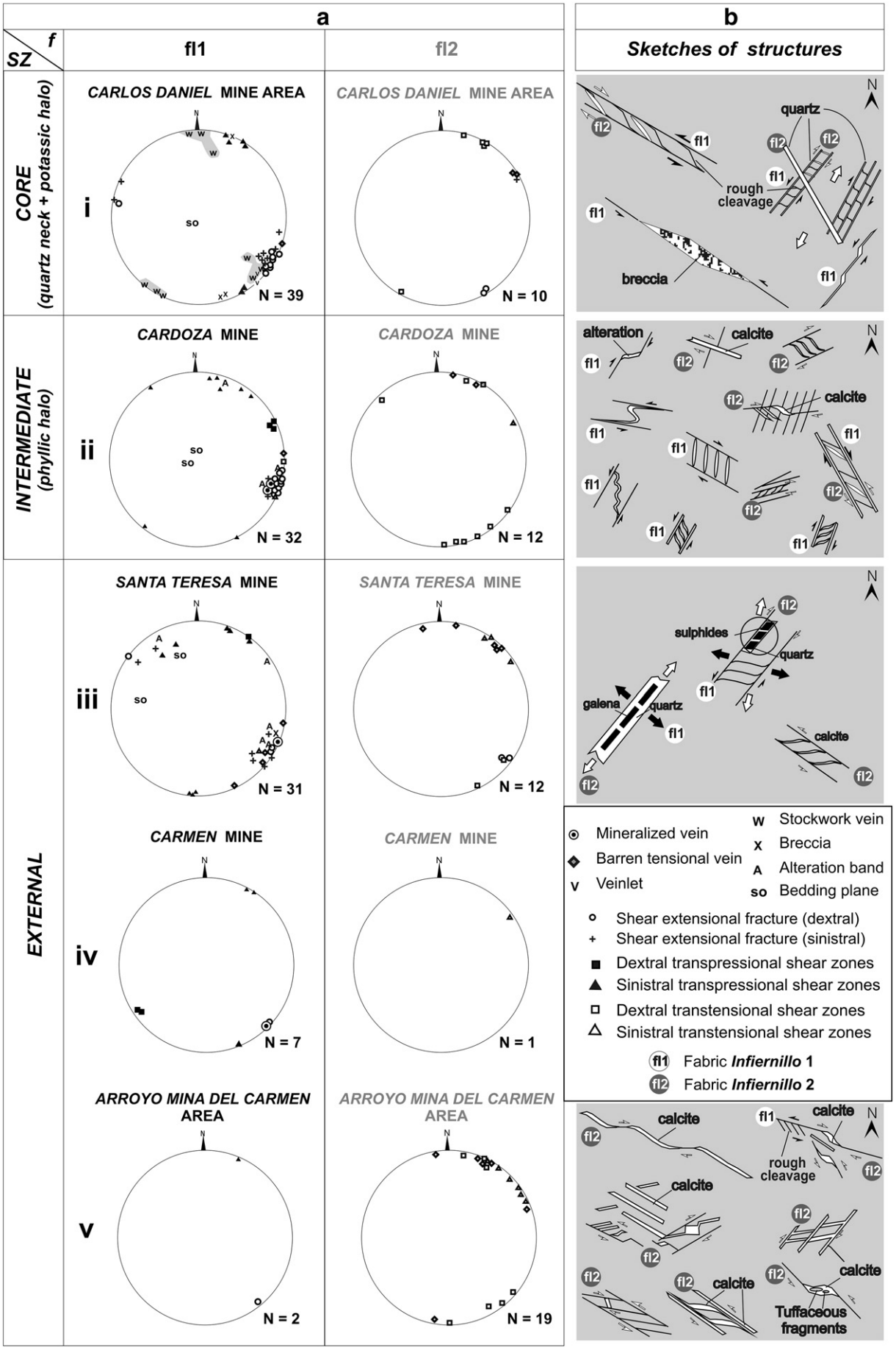
a
b
SZ
f
fl1
fl2
Sketches of structures
CORE
(quartz neck + potassic halo)
INTERMEDIATE
(phyllic halo)
EXTERNAL
CARLOS DANIEL MINE AREA
i
N = 39
N = 10
CARDOZA MINE
ii
N = 32
N = 12
SANTA TERESA MINE
iii
N = 31
N = 12
CARMEN MINE
iv
N = 7
N = 1
ARROYO MINA DEL CARMEN AREA
v
N = 2
N = 19
quartz
rough cleavage
breccia
alteration
calcite
sulphides
galena
Tuffaceous fragments
Mineralized vein
Barren tensional vein
Veinlet
Stockwork vein
Breccia
Alteration band
Bedding plane
Shear extensional fracture (dextral)
Shear extensional fracture (sinistral)
Dextral transpressional shear zones
Sinistral transpressional shear zones
Dextral transtensional shear zones
Sinistral transtensional shear zones
Fabric Infiernillo 1
Fabric Infiernillo 2

5.2. Las Picazas mine

The Early Paleozoic host rocks of *Las Picazas* (La Horqueta Formation) show at least three different strain fabrics (fLP1, fLP2, fLP3; Fig. 7a). The first one (fLP1) is represented by ductile structures such as SW-striking transected folds (according to Borradaile, 1978), with SE-vergence and axes plunging 235°–240°/30°. fLP1 also involves NNW to NNE (350°–010°/35°–45°W) striking cleavage (Fig. 6f) as well as a variable stretching lineation, and strongly folded quartz veins. The younger two fabrics (fLP2 and fLP3) deform the older fLP1 and are represented by brittle–ductile transpressional structures (fLP2: WNW sinistral and NNW dextral), transtensionally reactivated (fLP3: WNW dextral and NNW sinistral; Figs. 6g and 7a), both with associated tensional structures. Post-fLP1 tensional structures involve pre-mineralization (NNE 040°) and syn-mineralization *La Picaza* and *La Juanita* veins (NW 135°–145°/70°W; Figs. 7a and biii).

Kinematic indicators in the *La Juanita* and *La Picaza* mineralized veins show a predominant component of vertical (dip) displacement and subordinate components of dextral and sinistral motions, implying a NE–NNE direction of extension during vein emplacement. Some *en-échèlon* tensional gashes overprint some of these veins (Fig. 7biii) and show sinistral component of motions.

Near the mineralized veins, a first generation of barren, WNW striking shear extensional veins and breccias (Az 105°–110°) are found. A second generation of barren, NW veins (Az. 125°–136°) showing quartz comb-texture developed within this WNW dextral set. Sinistral transtensional, brittle–ductile shear zones striking NNW (165°–180°) are also present in the surrounding area (Fig. 7a and biv).

At about 1.5 km to the southeast of *Las Picazas* (*Las Picazas* S, Fig. 3d) three veins striking WNW to NW (125°–135°/80° NE) follow a horse tail design in the horizontal plane. They show similar strain fabric and 2-D kinematic frame as the *La Juanita* and *La Picaza* veins (Fig. 7a): brittle–ductile transtensional shear zones strike WNW (110°, dextral) and NNW (140°–180°, sinistral), whereas tensional fractures strike NW (130°).

Farther to the southeast of Las Picazas, the *Agua del Pablito* veins (Figs. 1a and 3d) comprise two sets of NNW (170°/25°W) and WNW (112°/60°S) trending mineralized veins (Carpio et al., 2001).

6. Discussion

Deformation at both the *Infiernillo* and *Las Picazas* deposits is strongly heterogeneous in character. Brittle–ductile shear zones are inhomogeneously distributed all around these areas and the anisotropic nature of the host rock seems to be crucial. The main structural trends are coincident with the WNW to ENE and NW-trending Grenvillian structures recognized in well exposed outcrops of Sierra Pie de Palo, ~330 km to the NNE of San Rafael (Ramos et al., 2000), and NNW-striking structures that are representative of the structural grain linked to the suture zone involving the collision of the Chilenia terrane (W) to the Pacific side of Cuyania (E) by the end of the Devonian (Ramos, 2004). This main control is reflected in the high partitioning of motions (Kleiman and Japas, 2009).

6.1. Infiernillo and Las Picazas strain fabrics

In order to analyze the strain fabric of both ore deposits, a summary of the main fabric elements shown in Figs. 5 and 7 (fl1, fl2, fLP3) is represented in Fig. 8.

The results from fl1 set are shown in Fig. 8a. WNW sinistral transpressional brittle–ductile shear zones are present in all the studied *Infiernillo* localities. The four sets of the shear structures measured at *Carlos Daniel* mine area are coincident with the main sets of the nearly-radial system of fractures represented in Fig. 4a. The kinematic significance of the shear-extensional structures is uncertain. However, outside the core zone, shear-structures seem to be more consistent. NNW–NW dextral transpressional brittle–ductile shear zones were significantly recognized at *Cardoza* and *Carmen* mines (Fig. 8a), very close to the eastern margin of the proposed NNW dextral transpressional structure that controls the three silicification zones (see Fig. 4b). These would be the result of localized shear related to this NNW structure.

Considering fl2, the dextral transtensional kinematic of WNW structures is consistent in all the measured localities (Fig. 8a) where an equivalent ENE population is also present. Although NNW to NW-striking brittle–ductile shear zones are not well represented in all the selected areas, they show sinistral transtensional motions (Fig. 8a). These sinistral transtensional structures are predominant at the *Arroyo Mina del Carmen* area (the best developed fl2 fabric of this ore deposit) where they show some degree of overlapping with those WNW shear zones that show dextral transtensional kinematics.

When all the fl1 diagrams are superposed together (Fig. 8b), it is evident that the WNW sinistral transpressional set is dominant and that the NNW dextral one comprises a subordinated group. A characteristic pattern of shear extensional fractures reveals NNE overlapping of dextral and sinistral structures with the dextral structures orientated at lower Azimuth than sinistral structures. This can be interpreted as the consequence of rotation linked to sinistral WNW shearing (Fig. 8c). The higher angle between the WNW-striking shear boundary and the NNE convergence direction calculated by Kleiman and Japas (2009) induces the higher angle between the deformed zone and the Riedel shear/tensional fracture system. This is because in a transpressional regime, the component of shortening orthogonal to the shear zone causes the long axis of the horizontal strain ellipse to develop at lower angles to the zone boundaries than in simple shear strike–slip (Ghosh and Chattopadhyay, 2008; Sanderson and Marchini, 1984; Schreurs and Colletta, 1998). This causes Riedel shears and tensional fractures to develop at high angles to the bounding zones (e.g. $\delta > 45°$ for tensional fractures; case 3 in Fig. 2a). This is evident at *Santa Teresa*–San *Francisco* and *Cardoza* areas where WNW sinistral brittle–ductile shear zones are the predominant transpressional structures (Fig. 5aii–iii). In this way, some dispersion in vein and fracture trends (Figs. 5a and 8c) could be explained as an effect of a counter-clockwise rotation during progressive, sinistral, non-coaxial deformation (see Bons et al., 2012; Fig. 8c). With rotation of tensional fractures, they were converted into sheared extensional fractures (Fig. 8c) and then they become progressively misoriented to accommodate extension and may themselves be deformed by the development of new, more ideally oriented, tensional structures (Fig. 8c). The asymmetric and localized distribution of

Fig. 5. Minor structures from *Infiernillo* area. a. Equal-area stereonet plots of main structural elements (lower-hemisphere). SZ: Structural zones based on differences in structural grain. f: Fabric. Two diagrams are presented for each locality since minor structures can be grouped following two fabrics: fl1 (left plots) and fl2 (right plots). At *Infiernillo*, fl2 elements commonly appear reactivating fl1 elements. Despite the mines sharing common strain fabric elements, strain at *Infiernillo* is heterogeneous resulting in a different degree of minor-structures development per area. In the *Carlos Daniel* plot, shaded areas representing the main stockwork fracture trends are shown. Scarce NNW dextral transpressional structures are also present (but not represented as no dip could be measured). The *Santa Teresa* plot comprises both, *Santa Teresa* and *San Francisco* mine data. Dissimilar frequency of structures at each locality confirms the heterogeneous character of deformation. b. Schematic sketches (metric to decimetric scale) of fl1 and fl2 minor structures observed at the analyzed *Infiernillo* localities. These sketches show geometrical patterns of minor structures, kinematic indicators with inferred motions and timing of both fabrics. Boundaries of brittle–ductile transpressional/transtensional shear zones are represented by parallel straight lines. Some brittle–ductile transpressional shear zones display rough cleavage (including sigmoidal cleavage) represented by black lines. In white, dilatational structures (veins and dilatational jogs) are represented. Black arrows indicate fl1 extension direction; white arrows indicate fl2 direction of extension; pairs of black hemi-arrows indicate shear motions for the represented fl1 structure; pairs of white hemi-arrows indicate shear motions for the represented fl2 structure. Sketches are scale independent.

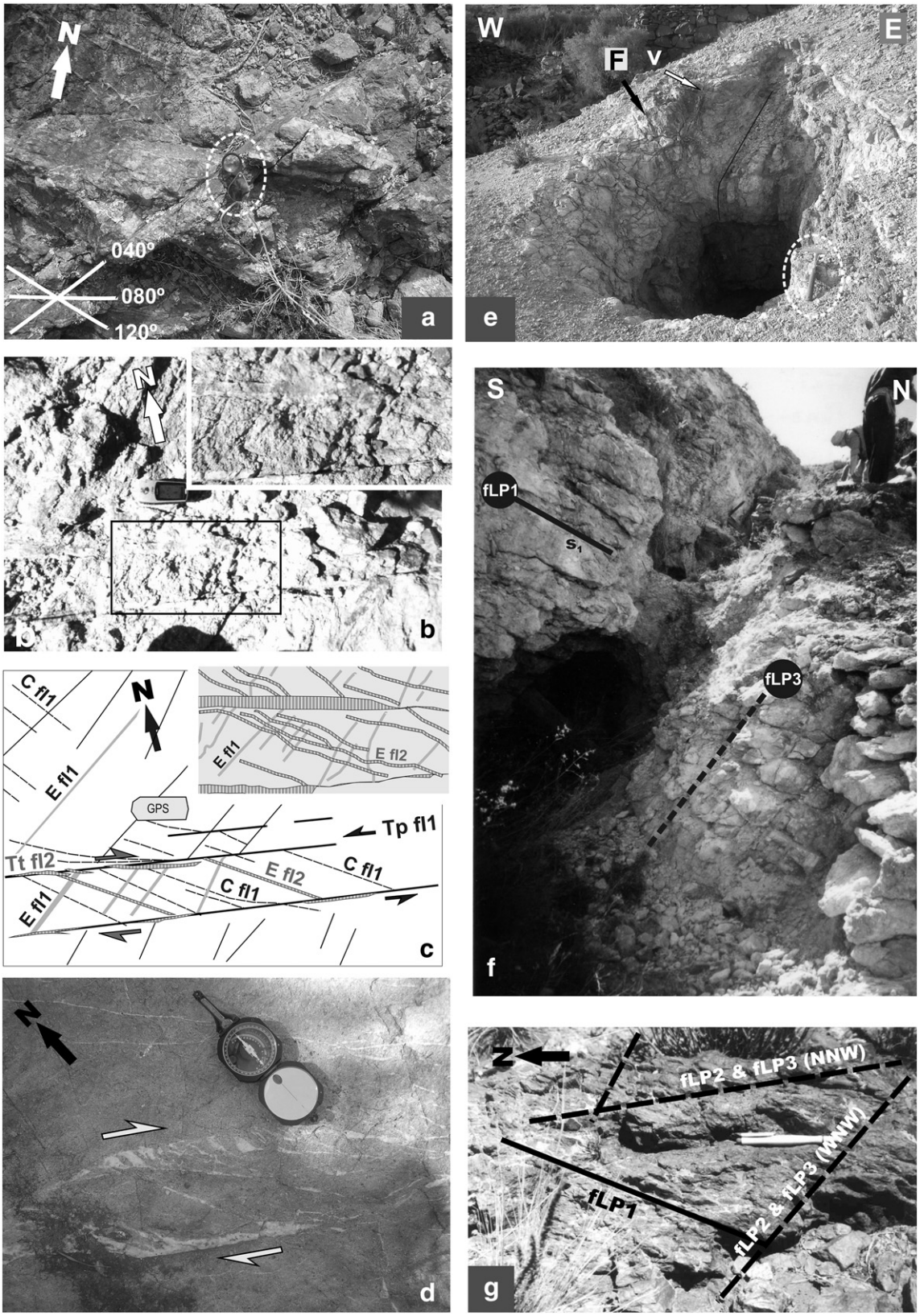

Fig. 6. Structural fabric elements. a. Stockwork at the *Carlos Daniel* area (magnifying-glass for scale). Three preferred fracture trends are predominant (Azs 040°, 080°, 120°). b. Az 110° sinistral transpressional San Rafael Orogeny shear zone affecting lower Choiyoi pyroclastites in the potassic halo. A notable NNE extensional penetrative fabric can be appreciated. Enlargement of the rectangle area is presented top-right of the figure. c. Sketch of the previous plate. The relationship between brittle–ductile transpressional and transtensional shear zones could be observed. fl1 fabric elements: Tp fl1: transpressional zone; C fl1: contractional structures; E fl1: tensional structures (filled by quartz). fl2 fabric elements: Tt fl2: transtensional reactivated zone; E fl2: extensional structures (overprinted and filled by calcite). d. fl2 brittle–ductile transtensional shear zone in the *Cardoza Oeste* Mine area. e. Mineralized vein at the *Santa Teresa* mine (hammer for scale). F: fracture; V: vein. f. *Las Picazas* area showing the host rock (La Horqueta Fm. metaschists) with a strong planar fabric (s_1 350°–010°/35°–45°W; fLP1) overprinted by a parallel-to-the-vein fracture fabric (fLP3). g. Fabric of La Horqueta Fm. (Early Paleozoic) rocks near *Las Picazas* deposit. Solid line indicates cleavage of La Horqueta Fm. schists (fLP1). Dashed lines remark structures representing transpressional (fLP2) and reactivated transtensional (fLP3) main fabric directions.

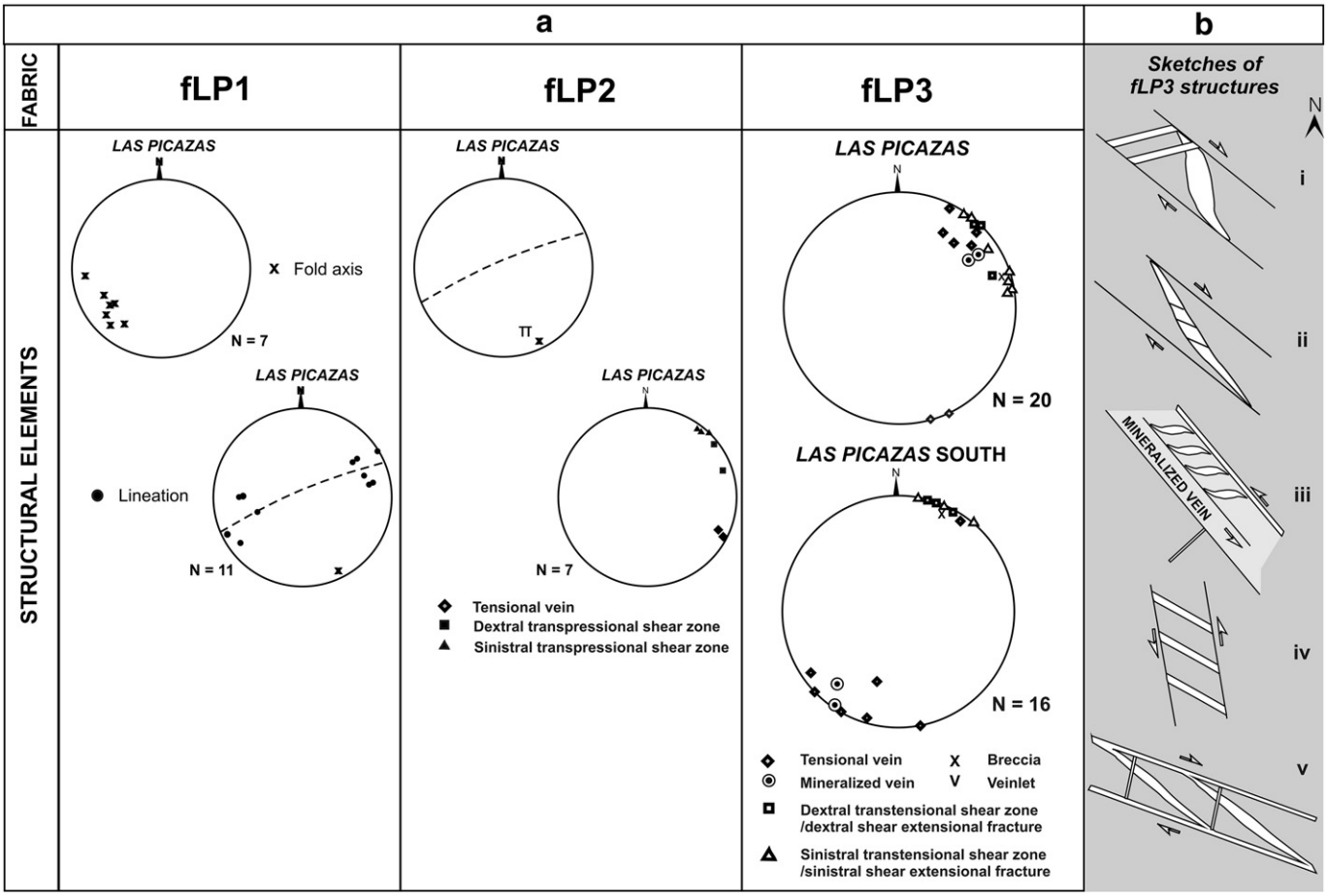

Fig. 7. Overprinted fabrics in La Horqueta Formation rocks at *Las Picazas* area. a. Equal-area stereonet plots of main structural elements (lower-hemisphere) considering the three different recognized fabrics (fLP1, fLP2, fLP3). b. Sketches of tensional and shear extensional veins related to brittle–ductile transtensional shear zones of metric to decimetric scale. Kinematic indicators and inferred motions are shown. Geometries of veins and arrays of veins: *en-échèlon* (iii, iv, v), sigmoidals (i, ii, iii), straight (iv, v) and *boudined*-like (iii, defined by "*boudins*" of the main vein formed as a consequence of a second generation of sigmoidal syn-mineralization veins). The latter case (iii) would reveal transtensional reactivation of the main tensional vein as the result of vein rotation during non-coaxial deformation. (i), (ii) and (v) show mineralized veins associated with secondary post-mineralization veins. (i), (ii) and (v) belong to dextral WNW bands whereas (iii) and (iv) belong to sinistral NNW bands.

mineralized veins (Fig. 4a) would also support this non-coaxial model as they would indicate favorable pathways changing during the history of the hydrothermal system (see Jiang et al., 1997), enhancing asymmetrical fracture connectivity.

The plot of the all the entire fl2 shear-structures diagrams reveals principal dextral transtensional and shear extensional structures striking WNW and ENE. The sinistral transtensional set trends NNW–NW and partially overlaps the dextral set. This could also be attributed to non-coaxial deformation (Fig. 8c).

The results of strain fabric analysis performed both at the *Infiernillo* and at *Las Picazas* ore deposits should be analyzed within the regional context of the southwestern margin of Gondwana as Choiyoi magmatism recorded major geodynamic changes during the Permian (Japas and Kleiman, 2004; Kleiman and Japas, 2009). According to these authors, the Lower Choiyoi rocks emplaced syntectonically with the transpressional regime of the San Rafael Orogeny and display a San Rafael Orogeny fabric. This fabric resulted from NNE oblique convergence and consisted of NNE tensional and NW–WNW contractional structures in association with NNW dextral and WNW sinistral transpressional bands, which were reactivated by later Post-San Rafael structures produced by a change to a transtensional regime. Also, and as a consequence of their emplacement during the Post-San Rafael transtension, Upper Choiyoi volcanics are affected by Post-San Rafael structures which are represented by NW–WNW tensional fractures, NNW sinistral and WNW dextral transtensional structures.

According to Tosdal and Richards (2001) structural zoning of porphyry systems would indicate core rocks deforming as a consequence of magmatic pressure–tectonic stress interplay and peripheral cool rocks revealing fracturing under the influence of the regional field. At *Infiernillo*, both the peripheral tensional-to-shear-extensional veins and the maximum axis of the elliptical alteration zone strike NNE, in coincidence with regional San Rafael Orogeny tensional structures. Additionally, main brittle–ductile transpressional shear zones (fl1) also match with the San Rafael Orogeny fabric, since sinistral structures strike WNW (110°; Fig. 6c) and dextral structures strike NNW (150°). Moreover, although scarce, well preserved 3-D kinematic indicators linked to the mineralization stage also reveal San Rafael Orogeny kinematic axes (fl1 in Fig. 9a; see Kleiman and Japas, 2009).

Further evidence of mineralization occurring during the San Rafael Orogeny at *Infiernillo* includes: a) the presence of alteration bands and breccias coinciding with San Rafael Orogeny transpressional zones, b) the presence of *en-échèlon*-like pattern of silicified areas within the potassic halo (Fig. 4b), and c) the location of ore deposits at the intersection of two regional San Rafael Orogeny transpressional structures (WNW and NNW, Fig. 3a and c). These WNW and NNW San Rafael Orogeny trends were also interpreted using IP information (Japas and Rubinstein, 2006).

As described above, Post-San Rafael extension fabric is also present at *Infiernillo* (fl2, Figs. 5a, b, 8a and c). This is also supported by the mineralized vein striking NNE that is *boudinaged* revealing a late stage of

NNE extension (*San Francisco* mine; Fig. 5biii). Fuschini (1968) also described a late mineralizing stage represented by thin veins carrying Fe-oxides which is orthogonal to the main NNE mineralized vein system. Likewise, the transtensional array of late calcite veins suggest that Post-San Rafael strain fabric both reactivated and overprinted the San Rafael Orogeny structures (Fig. 6b and c). This reactivation/overprinting event is also supported by 3-D kinematic data (Fig. 9a, fl2 right plot). The presence of some andesitic dykes of the Quebrada del Pimiento Fm. (Upper Choiyoi) striking NNW and WNW (Fig. 4a; Gómez and Rubinstein, 2010) would confirm that the equivalent transtensional fabric elements recognized at *Infiernillo* are Post-San Rafael structures.

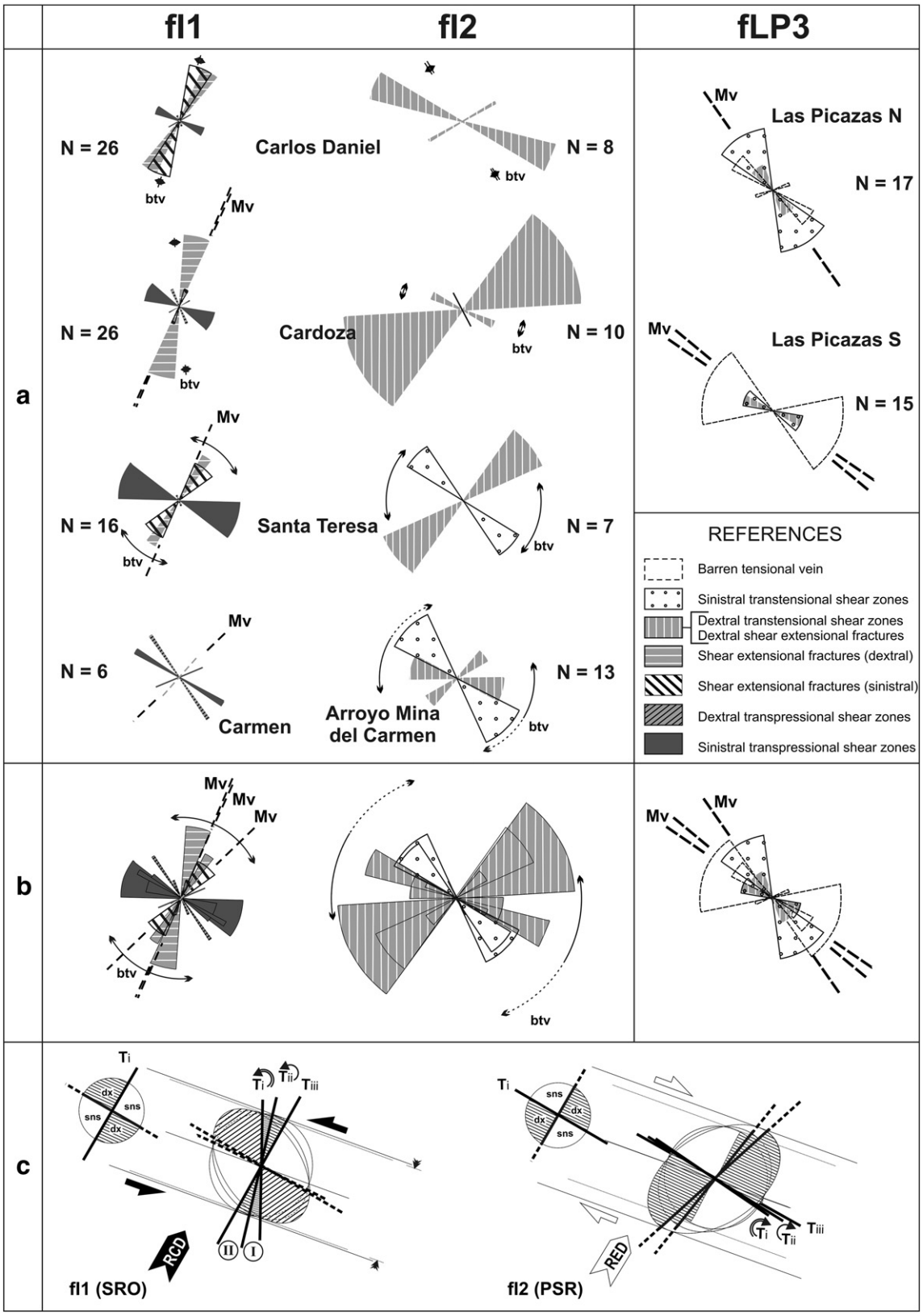

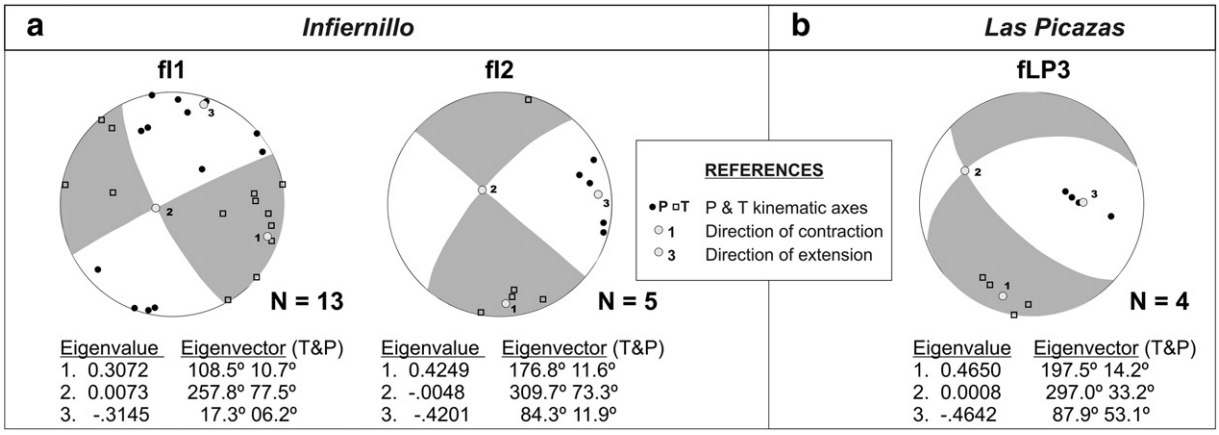

Fig. 9. Comparative kinematic data obtained by the kinematic "P" (shortening) and "T" (extension) axes method. The 3-D kinematic plots were calculated via Allmendinger's FaultKinWin Program (2001) and show the estimated kinematic axes for a. *Infiernillo* (fl1, left plot; fl2, right plot) and b. *Las Picazas* (fLP3) mineralized fabrics. "P" and "T" represent the principal infinitesimal shortening and extension axes for each measured structure respectively. Planes (nodal planes) bound two pairs of areas; the gray area represents the extension field whereas the white area refers to the shortening domain. Notice that although the data are scarce (see Arlegui-Crespo and Simón-Gómez, 1998), the results are consistent with previous published data: The shortening direction ("3") obtained for fl1is coincident with the direction that Kleiman and Japas (2009) consider as representative of the San Rafael Orogeny fabric. fl2 structures indicate a NNE extension direction ("1") in coincidence with the direction that Kleiman and Japas (2009) consider as representative of the Post-San Rafael extension fabric. In *Las Picazas* area, fLP3 extension direction ("1") is coincident with the Post-San Rafael extension direction defined by the same authors.

Strain fabrics fl1 and fl2 would indicate a main tectonic control performed by the regional WNW structure that defines the North Domain (Fig. 3a and b). This agrees not only with the predominance of WNW shear structures for both strain fabrics but also with paleomagnetic data results reported by Tomezzoli and Japas (2006) who interpreted clockwise tectonic block rotations linked to the Post-San Rafael regime at the Agua del Toro dam region that is located ~20 km WNW from *Infiernillo* (Fig. 1a).

This evidence points to a porphyry emplacement during the transition from San Rafael Orogeny transpression to Post-San Rafael transtension. Therefore, this porphyry system would have been emplaced at the time of Agua de los Burros Formation volcanism (Kleiman and Japas, 2009). This unit, which records the last stage of the San Rafael Orogeny, was dated at ~265 Ma (Rocha-Campos et al., 2011).

Concerning fLP3, mineralized veins at *Las Picazas* show an extensional imbricate fan design that results in different vein attitudes: NNW–NW to the north and WNW to the south (Fig. 8a). Concomitantly, sinistral and dextral transtensional brittle–ductile shear zones strike NNW and WNW, north and south respectively. While angular relationships between tensional barren veins and the transtensional structures at *Las Picazas* (north) confirm sinistral motions (Fig. 8a), the nearly symmetric distribution of structures at *Las Picazas S* would suggest a tensional array. This is concordant with a vein array geometry caused by the reactivation of previous structures. *Las Picazas* (north) shows predominant NNW-striking sinistral brittle–ductile shear zones but also some dextral transtensional ones.

When all the fLP3 diagrams are shown together, shear structures appear grouped into a main NNW sinistral transtensional array, partially overlapping the suite of dextral transtensional structures that trends WNW–NW (Fig. 8b). Mineralized veins support main NNW sinistral transtension.

Las Picazas mineralized veins are interpreted as NW-trending tensional to shear extensional fractures (130°–145°) and related to NNW (140°–160°, sinistral) and WNW (110°–120°, dextral) fLP3 transtensional zones (Figs. 3d and 7a), indicating that ore emplacement was controlled by Post-San Rafael extension. This is also supported by the extensional imbricate fan design (following Woodcock and Fischer, 1986) that the veins define (Fig. 3d). In *Las Picazas* case some dispersion in vein and fracture trends (Fig. 7, fLP3) as well as the presence of sinistral and dextral transtensional brittle–ductile shear zones displaying the same attitude, could be also explained as an effect of rotation during progressive noncoaxial deformation (Fig. 8c; see Fossen, 2010; Ghosh, 2001; Pollard and Fletcher, 2005; Ramsay, 1967).

Since a) fLP3 fabric overprinted and reactivated the transpressional fLP2 and b) both postdate fLP1, then fLP2 and fLP1 would be the result of the Early Permian San Rafael orogeny and a pre-Permian (Chanic) orogeny, respectively. Confirming this, fLP2 is concordant with the regional San Rafael Orogeny structural grain (fLP1 stretching lineation follow a great circle whose axis is coincident with the regional NNW San Rafael Orogeny folding lineation defined for its first orogenic stage by Kleiman and Japas, 2009; Fig. 7a), and the barren NNE veins (post-fLP1, pre-mineralization) show a notable parallelism with the fl1 tensional

Fig. 8. a. Synoptic rose diagrams showing main fractures and brittle–ductile shear zones associated with mineralization at *Infiernillo* (fl1 and fl2) and *Las Picazas* (fLP3) (summarized from Figs. 5a and 7a). Variable class intervals were selected in order to highlight the occurrence of specific groups of shear-structures at distinctive strike intervals. MV: mineralized vein, btv: interval for strikes of barren tensional veins at *Infiernillo*. b. Data from each fabric set were grouped into single diagrams in order to visualize the regional tendency. Single diagrams were simply superposed and frequency was not re-calculated. *Carlos Daniel* mine was excluded from the whole fl1 representation because of the presence of the mentioned structural zoning. c. Simplified sketch to clarify how the rotation of tensional fractures and shear extensional fractures under WNW sinistral transpressional (left) and WNW dextral transtensional (right) regimes could explain the coexistence of tensional (T) and dextral/sinistral shear-extensional fractures with the same strike. Also, sheared T fractures could be present, since T structures would be deformed once rotated. RCD: regional contractional direction; RED: regional extensional direction. Incremental strain ellipse (top) shows the fields in which shear related structures could develop. Ti, Tii, Tiii: tensional structures at the strain increments 1, 2 and 3, respectively. Left: As a consequence of strain increment 2, for example, those tensional structures developed at stage 1 (Ti) will rotate, and as a result of this new position they should be affected by shear. Notice that at different stages, new sets of tensional structures could materialize. Field I represents the attitude of those early sinistral shear extensional fractures (stage 1) that after rotation (increments 2 and 3) undergo dextral displacements. Field II refers to those sinistral shear extensional fractures (stage 2) that following strain increment 3 face dextral motions. Therefore, structures striking according to fields I and II should be characterized by the coexistence of tensional and shear extensional (sinistral and dextral) fractures. Coexistence of brittle–ductile shear zones showing different motions and the same attitude could be explained using the same progressive deformation concept.

structures observed at *Infiernillo*. As additional evidence, although scarce, well preserved 3-D kinematic indicators at *Las Picazas* would indicate Post-San Rafael kinematic axes (Fig. 9b).

NNW and WNW Post-San Rafael brittle–ductile shear zones at *Las Picazas* comprise then transtensional reactivations of San Rafael Orogeny structures that were re-sheared due to their optimal orientation that induced failure at much lower differential stresses than those required for newly-formed structures (see Sibson, 1998; Stephens et al., 2004). This would support a non-coaxial regime controlling vein emplacement and the consequent development of more-than-one generation of tensional veins/fractures as the result of progressive deformation (e.g.: the late generation of barren, NW veins showing quartz comb-texture developed within the main WNW set; Figs. 7biii and 8c).

Las Picazas could either be genetically related to the Late Permian Upper Choiyoi or to the Triassic Puesto Viejo volcanism since both sequences emplaced syntectonically with the Post-San Rafael extension.

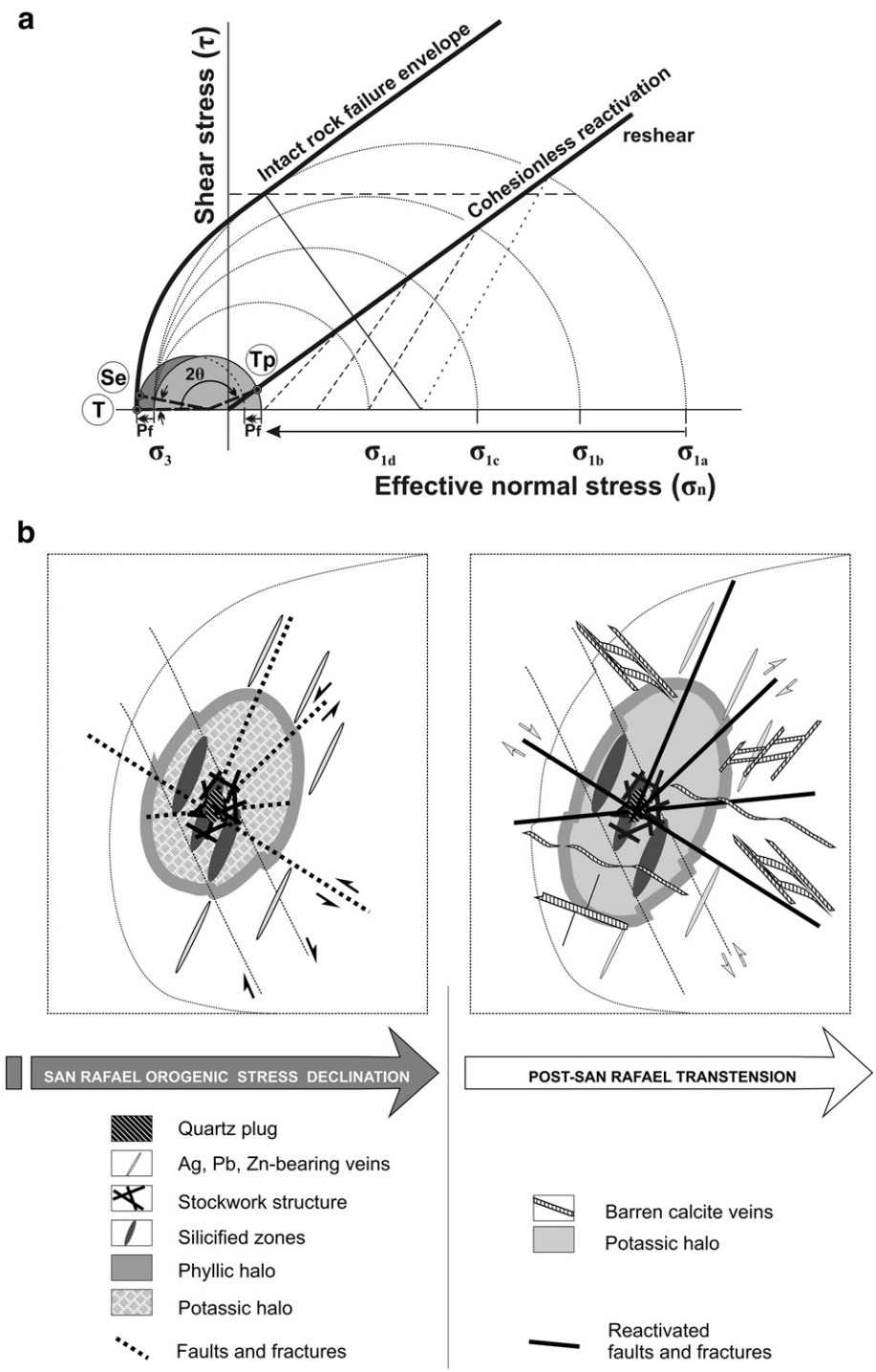

Fig. 10. a. Generic, schematic Mohr diagram showing the interpreted stress/fluid pressure conditions based on *Infiernillo* data (modified from Sibson, 1998; Stephens et al., 2004). Envelopes for intact rock and for frictional reactivation of an existing pre-Cochicó cohesionless fault are represented. Tp: Transpressional WNW structures controlled by previous structure. High pressure condition stage controlling peripheral vein emplacement; Pf: Fluid pressure; Se: shear-extensional; T: tensional structures. b. *Infiernillo* deposit evolution. Simplified sketch showing the relationships between ore deposit elements and structure (San Rafael Orogeny, and Post-San Rafael extension stages). Fault displacements of the phyllic halo are enhanced to visualize temporal relationships.

Thus, the maximum age for *Las Picazas* ore deposit should postdate the age of Agua de los Burros Formation and therefore be younger than 265 Ma.

6.2. Low-sulfidation epithermal/porphyry-type deposits and geodynamical setting

The emplacement of porphyry Cu deposits is generally related to stress relaxation conditions at the end of an orogeny (Billa et al., 2004; Tosdal and Richards, 2001). At the *Infiernillo* deposit, a waning contractional San Rafael Orogeny stress regime could be inferred based on the presence of sets of transpressional/tensional/shear extensional fractures (mixed-mode of fractures, Sibson, 1998). According to Cosgrove (1995) the coexistence of these fractures would indicate both supra-lithostatic fluid pressure (inducing hydraulic fracturing) and declining stress conditions (see Fig. 10a). Moreover, the presence of a structural zoning would also support the waning of the San Rafael Orogeny (see Tosdal and Richards, 2001). Although these indirect lines of evidence support the proposed relationship between stress relaxation and Cu-porphyry deposits, strain fabric data at *Infiernillo* offer additional, measurable evidence of an association between Cu-porphyry deposits and waning orogenic systems as they reveal the change in the stress regime: an early stage of mineralization that occurred under transpression of the San Rafael Orogeny was followed by a late stage of carbonatization, controlled by Post-San Rafael extension (Fig. 10b).

7. Conclusions

The present strain fabric analysis confirms previous proposals of Billa et al. (2004), Sillitoe and Hedenquist (2003), and Tosdal and Richards (2001) about the main role of the tectonic regime in controlling hydrothermal mineralization style, since it demonstrates that mineralization at *Infiernillo* (Cu–Mo porphyry-type deposit) was controlled by transpressional San Rafael Orogeny structures whereas mineralization at *Las Picazas* (low-sulfidation epithermal veins) was controlled by transtensional Post-San Rafael structures. Moreover, strain fabric data at *Infiernillo* record the change in the tectonic regime, confirming that porphyry emplacement occurs during a waning transpressional (compressional) tectonic regime.

Strain fabric analysis proves to be a simple, low-cost tool that a) contributes to the analysis and discrimination of ore deposits emplaced under different geodynamical settings, b) allows the identification of different stages during ore deposits evolution, and c) helps to examine the incidence of the regional and the local tectonic controls.

Acknowledgments

The authors wish to thank F. Carpio, E. Zappettini, and C. Balmaceda, as well as the Servicio Geológico Minero de Argentina (SEGEMAR) for their support during the fieldwork. Also thanks go to A. Gómez and A. Archangelsky for the help received with photographs, to R. Allmendinger for free access to the FaultKinWin software and to David Edwards for language revision of the previous draft. We are grateful to Dr. Stephan White and an anonymous reviewer for their fruitful corrections and suggestions.

Appendix A. Supplementary data

Supplementary data associated with this article can be found in the online version, http://dx.doi.org/10.1016/j.oregeorev.2013.01.018. These data include Google map of the most important areas described in this article.

References

Allmendinger, R.W., 2001. FaultKinWin, version 1.1. A program for analyzing fault slip data for Windows™ computers. http://www.geo.cornell.edu/geology/faculty/RWA/programs.html.
Arlegui-Crespo, L.E., Simón-Gómez, J.L., 1998. Reliability of palaeostress analysis from fault striations in near multidirectional extension stress fields. Example from the Ebro Basin, Spain. J. Struct. Geol. 20, 827–840.
Becker, A., Gross, M.R., 1999. Sigmoidal wall-rock fragments: application to the origin, geometry and kinematics of en échelon vein arrays. J. Struct. Geol. 21, 703–710.
Billa, M., Cassard, D., Lips, A.L.W., Bouchot, V., Tourlière, B., Stein, G., Guillou-Frottier, L., 2004. Predicting gold-rich epithermal and porphyry systems in the Central Andes with a continental-scale metallogenic GIS. Ore Geol. Rev. 25, 39–67.
Blundell, D., Arndt, N., Cobbold, P., Heinrich, Ch., 2005. Processes of tectonism, magmatism and mineralization: lessons from Europe. Ore Geol. Rev. 27, 333–349.
Bons, P.D., Elburg, M.A., Gómez-Rivas, E., 2012. A review of the formation of tectonic veins and their microstructures. J. Struct. Geol. 43, 33–62.
Borradaile, G.J., 1978. Transected folds: a study illustrated with examples from Canada and Scotland. Geol. Soc. Am. Bull. 89, 481–493.
Carpio, F.W., 1999. El yacimiento polimetálico Río Diamante, Mendoza. In: Zappettini, E.O. (Ed.), Recursos Minerales de la República Argentina. Instituto de Geología y Recursos Minerales, pp. 877–879.
Carpio, F., Mallimacci, H., Rubinstein, N., Salvarredi, J., Sepúlveda, E., Centeno, R., Rosas, M., Vargas, D., 2001. Metalogenia del Bloque de San Rafael, Mendoza. Serv. Geol. Min. Argent., Serie Contribuciones Técnicas, Recursos Minerales (109 pp.).
Chardon, D., Peucat, J.J., Jayananda, M., Choukroune, P., Fanning, C.M., 2002. Archean granite–greenstone tectonics at Kolar (South India): interplay of diapirism and bulk inhomogeneous contraction during juvenile magmatic accretion. Tectonics 21, 1–16. http://dx.doi.org/10.1029/2001TC901032.
Clark, D.A., 1999. Magnetic petrology of igneous intrusions: implications for exploration and magnetic interpretation. Explor. Geophys. 30, 5–26.
Cortés, J.M., Japas, M.S., Pasini, M., 2009. El hemigraben triásico Paramillos, Precordillera sur mendocina. Congr. Geol. Argent. Abstracts, Jujuy, Argentina, 3, pp. 1279–1280.
Cosgrove, J.W., 1995. The expression of hydraulic fracturing in rocks and sediments. In: Ameen, M.S. (Ed.), Fractography: Fracture Topography as a Tool in Fracture Mechanics and Stress Analysis: Geol. Soc. Lond. Spec. Publ., 92, pp. 187–196.
Delpino, D., 1997. Geología regional y petrología del Complejo Los Corrales paleozoico superior-triásico, provincia de Mendoza. Unpublished PhD thesis, Universidad de La Plata, La Plata.
Delpino, D., Pezzutti, N., Godeas, M., Donnari, E., Carullo, M., Núñez, E., 1993. Un cobre porfírico paleozoico superior en el centro volcánico San Pedro, distrito minero El Nevado, Provincia de Mendoza. Int. Congr. Carbonif. Permian CR, Buenos Aires, Argentina, 1, pp. 477–490.
Dewey, J.F., Holdsworth, R.E., Strachan, R.A., 1998. Transpression and transtension zones. In: Holdsworth, R.E., Strachan, R.A., Dewey, J.F. (Eds.), Continental Transpressional and Transtensional Tectonics: Geol. Soc. Lond. Spec. Publ., 135, pp. 1–14.
Di Tommaso, I., Rubinstein, N.A., 2007. Hydrothermal alteration mapping using ASTER data in the Infiernillo porphyry deposit, Argentina. Ore Geol. Rev. 32, 275–290.
Fossen, H., 2010. Structural Geology. Cambridge University Press, Cambridge.
Fossen, H., Tikoff, B., 1998. Extended models of transpression and transtension, and application to tectonic settings. In: Holdsworth, R.E., Strachan, R.A., Dewey, J.F. (Eds.), Continental Transpressional and Transtensional Tectonics: Geol. Soc. Lond. Spec. Publ., 135, pp. 15–33.
Fuschini, M., 1968. Informe final Área de Reserva No 26. Zona: Infiernillo. Plan Cordillerano. Serv. Geol. Min. Argent. (33 pp.).
Gargiulo, M.F., Rubinstein, N.A., Carpio, F., Salvarredi, J., 2007. Caracterización de la zona de alteración Central II, Bloque San Rafael, provincia de Mendoza. Rev. Asoc. Geol. Argent. 62, 387–395.
Ghosh, S.K., 2001. Types of transpressional and transtensional deformation. In: Koyi, H.A., Mancktelow, N.S. (Eds.), Tectonic Modeling: a Volume in Honor of Hans Ramberg: Geol. Soc. Am. Mem., 193, pp. 1–20.
Ghosh, N., Chattopadhyay, A., 2008. The initiation and linkage of surface fractures above a buried strike–slip fault: an experimental approach. J. Earth Syst. Sci. 117, 23–32.
Gómez, A., 2008. Geología del Deposito el Infiernillo, Bloque de San Rafael, Mendoza. Unpublished M.Sc. thesis, Universidad de Buenos Aires, Buenos Aires.
Gómez, A., Rubinstein, N.A., 2008. Mineralogía de las vetas de Mina Rosarito, Distrito Minero Infiernillo, Bloque de San Rafael, Mendoza, Argentina. In: Koukharsky, M., Montenegro, T., Poma, S., Quenardelle, S. (Eds.), Avances en Mineralogía, Metalogenia y Petrología, pp. 39–42.
Gómez, A., Rubinstein, N., 2010. Caracterización genética del Distrito Minero El Infiernillo, Bloque de San Rafael, provincia de Mendoza. Rev. Asoc. Geol. Argent. 67, 231–238.
González Díaz, E.F., 1973. Descripción geológica de la Hoja 27d, San Rafael, provincia de Mendoza. Serv. Nac. Min. Geol. 132 (127 pp.).
Hancock, P.L., 1985. Brittle microtectonics: principles and practice. J. Struct. Geol. 7, 437–457.
Hobbs, B.E., Means, W.D., Williams, P.F., 1976. An Outline of Structural Geology. Wiley, New York.
Japas, M.S., Tomezzoli, R.N., 2001. Cinemática neopaleozoica del Bloque de San Rafael, provincia de Mendoza. Simp. Argent. Paleoz. Super. Conference Abtracts, Trelew, Argentina, p. 14.
Japas, M.S., Kleiman, L.E., 2004. El Ciclo Choiyoi en el Bloque de San Rafael: de la orogénesis tardía a la relajación mecánica. Asoc. Geol. Argent. Pub. Spec. 7, 89–100.
Japas, M.S., Rubinstein, N.A., 2006. Informe estructural, Distritos mineros Infiernillo y Las Picazas. Hoja Minero — Metalogenética embalse Nihuil, Bloque de San Rafael, provincia de Mendoza. Unpublished report to Serv. Geol. Min. Argent., 15 pp.

Japas, M.S., Cortés, J.M., Pasini, M., 2008. Tectónica extensional triásica en el sector norte de la cuenca Cuyana, Precordillera Sur: Primeros datos cinemáticos. Rev. Asoc. Geol. Argent. 63, 213–222.
Japas, M.S., Urbina, N.E., Sruoga, P., 2010. Control estructural en el emplazamiento de rocas volcánicas y mineralizaciones neógenas, distrito Cañada Honda, San Luis, Argentina. Rev. Asoc. Geol. Argent. 67, 494–506.
Jiang, Z., Oliver, N., Barr, T.D., Power, W.L., Ord, A., 1997. Numerical modeling of fault-controlled fluid flow in the genesis of tin deposits of the Malage Ore Field, Gejiu Mining District, China. Econ. Geol. 92, 228–247.
Johanis, P., 2003. Geofísica Aérea Infiernillo. Unpublished report to Serv. Geol. Min. Argent., 5 pp.
Jurković, I., Palinkaš, L.A., 2002. Discrimination criteria for assigning ore deposits located in the Dinaridic Paleozoic–Triassic formations to Variscan or Alpidic metallogeny. In: Blundell, D.L., Neubauer, F., von Quadt, A. (Eds.), The Timing and Location of Major Ore Deposits in an Evolving Orogen: Geol. Soc. Lond. Spec. Publ., 204, pp. 229–245.
Kleiman, L.E., 1993. El volcanismo permo-triásico y triásico del Bloque de San Rafael (provincia de Mendoza): su potencial uranífero. Congr. Geol. Argent. Abstracts, Mendoza, Argentina, 5, pp. 284–293.
Kleiman, L.E., 1999. Mineralogía y petrología del volcanismo permo-triásico y triásico del Bloque de San Rafael en el área de Sierra Pintada, provincia de Mendoza, y su relación con las mineralizaciones de uranio. Unpublished PhD thesis, Universidad de Buenos Aires, Buenos Aires.
Kleiman, L.E., 2002. Movilidad de los elementos durante la alteración en dos mineralizaciones de U permotriásicas, San Rafael, Mendoza. Congr. Geol. Argent. Abtsracts, Calafate, Argentina, 2, pp. 300–304.
Kleiman, L.E., Japas, M.S., 2002. The lower Choiyoi volcanic sequence at 34°–35° 30′, San Rafael, Mendoza, Argentina: evidence of active plate convergence. Gondwana Meet. Abstracts, Christchurch, New Zealand (1p.).
Kleiman, L.E., Japas, M.S., 2009. The Choiyoi volcanic province at 34–36°S (San Rafael, Mendoza, Argentina): implications for the late Palaeozoic evolution of the south-western margin of Gondwana. Tectonophysics 473, 283–299. http://dx.doi.org/10.1016/j.tecto.2009.02.046.
Kleiman, L.E., Salvarredi, J.A., 2001. Petrología, geoquímica e implicancias tectónicas del volcanismo triásico (Formación Puesto Viejo), bloque de San Rafael, Mendoza. Rev. Asoc. Geol. Argent. 56, 559–570.
Korzeniewski, L.I., Gómez, A., Rubinstein, N.A., 2008. Estudio preliminar de inclusiones fluidas del pórfiro El Infiernillo, Mendoza, Argentina. In: Koukharsky, M., Montenegro, T., Poma, S., Quenardelle, S. (Eds.), Avances en Mineralogía, Metalogenia y Petrología, pp. 141–144.
Lenauer, I., Riller, U., 2012. Strain fabric evolution within and near deformed igneous sheets: the Sudbury Igneous Complex, Canada. Tectonophysics 558–559, 45–57.
Lisle, R.J., Vandycke, S., 1996. Separation of multiple stress events by fault striation analysis: an example from Variscan and younger structures at Ogmore, South Wales. J. Geol. Soc. 153, 945–953.
Llambías, E.J., Kleiman, L.E., Salvarredi, J.A., 1993. El magmatismo gondwánico. In: Ramos, V.A. (Ed.), Geología y recursos naturales de Mendoza, pp. 53–64.
Mann, P., 2007. Global catalogue, classification and tectonic origins of restraining- and releasing bends on active and ancient strike–slip fault systems. In: Cunningham, W.D., Mann, P. (Eds.), Tectonics of Strike–Slip Restraining and Releasing Bends: Geol. Soc. Lond. Spec. Publ., 290, pp. 13–142.
Mitchell, A.H.G., Garson, M.S., 1981. Mineral Deposits and Global Tectonic Setting. Academic Press, London.
Narciso, V., Zanettini, J.C., Sepúlveda, E., Mallimacci, H.S., 2007. Hoja Geológica 3769-II Agua Escondida. Serv. Geol. Min. Argent., 300 (54 pp.).
Olson, J.E., Pollard, D.D., 1991. The initiation and growth of en échelon veins. J. Struct. Geol. 13, 595–608.
Passchier, C.W., Trouw, R.A.J., 1996. Microtectonics. Springer-Verlag, Heidelberg.
Peacock, D.C.P., 1991. A comparison between the displacement geometries of veins and normal faults at Kilve, Somerset. Read. Ann. Conf. Ussher Soc. , pp. 363–367.
Pereira, J., Dixon, C.J., 1971. Mineralization and plate tectonics. Miner. Deposita 6, 404–405.
Pollard, D.D., Fletcher, R.C., 2005. Fundamentals of Structural Geology. Cambridge University Press, Cambridge.
Ramos, V.A., 2004. Cuyania, an exotic block to Gondwana: review of a historical success and the present problems. Gondwana Res. 7, 1009–1026.
Ramos, V.A., Vujovich, G.I., Cardó, R., Pérez, L., Pelichotti, R., Godeas, M., Pucci, J.C., 2000. Hoja Geológica 3169-IV San Juan. Serv. Geol. Min. Argent. Instituto de Geología y Recursos Minerales, 243 (82 pp.).
Ramsay, J.G., 1967. Folding and Fracturing of Rocks. Mc Graw-Hill, New York.
Ramsay, J.G., Huber, M.I., 1987. The Techniques of Modern Structural Geology. Folds and Fractures, Vol. 2. Academic Press, London.
Rocha-Campos, A.C., Basei, M.A., Nutman, A.P., Kleiman, L.E., Varela, R., Llambías, E., Canile, F.M., da Rosa, O.C.R., 2011. 30 million years of Permian volcanism recorded in the Choiyoi igneous province (W Argentina) and their source for younger ash fall deposits in the Paraná Basin: SHRIMP U–Pb zircon geochronology evidence. Gondwana Res. 19, 509–523.
Rubinstein, N.A., Gargiulo, M.F., 2005. Análisis textural de cuarzo hidrotermal del depósito El Pantanito, provincia de Mendoza: nuevos aportes sobre su génesis. Rev. Asoc. Geol. Argent. 60, 96–103.
Rubinstein, N., Mallimacci, H., Carpio, F., 2001. La mineralización epitermal del Pantanito, provincia de Mendoza, Argentina. Rev. Inst. Geol. Min. 14, 59–61.
Rubinstein, N., Carpio, F., Mallimacci, H., 2002a. Las vetas polimetálicas del área del Cerro San Pedro, provincia de Mendoza, Argentina. Congr. Geol. Argent. Abstracts, Calafate, Argentina, 2, pp. 263–266.
Rubinstein, N., Carpio, F., Mallimacci, H., 2002b. La zona de alteración del cerro Tres Hermanos, Mendoza, Argentina. In: Brodtkorb, M., Leal, P.A. (Eds.), Mineralogía y Metalogenia, pp. 419–420.
Rubinstein, N.A., Ostera, H., Mallimacci, H.S., Carpio, F., 2004. Lead isotopes from gondwanic ore polymetallic vein deposits, San Rafael Massif, Argentina. J. S. Am. Earth Sci. 16, 595–602.
Rubinstein, N.A., Morello, O., Japas, M.S., 2008. Caracterización de las vetas de Mina Picazas, Bloque de San Rafael, provincia de Mendoza. In: Koukharsky, M., Montenegro, T., Poma, S., Quenardelle, S. (Eds.), Avances en Mineralogía, Metalogenia y Petrología. Buenos Aires, pp. 159–162.
Rubinstein, N.A., Gómez, A., Mallimacci, H., 2012. La zona de alteración Arroyo La Chilca-Zanjón del Buitre, bloque de San Rafael, Mendoza. Rev. Asoc. Geol. Argent. 69, 287–295.
Sanderson, D.J., Marchini, D., 1984. Transpression. J. Struct. Geol. 6, 449–458.
Schreurs, G., Colletta, B., 1998. Analogue modeling in zones of continental transpression and transtension. In: Holdsworth, R.E., Strachan, R.A., Dewey, J.F. (Eds.), Continental Transpressional and Transtensional Tectonics: Geol. Soc. Lond. Spec. Publ., 135, pp. 59–79.
Sepúlveda, E., Bermúdez, A., Bordonaro, O., Delpino, D., Mallimacci, H.S., 2007a. Hoja Geológica 3569-IV Embalse El Nihuil. Serv. Geol. Min. Argent. 268 (52 pp.).
Sepúlveda, E., Carpio, F., Regairaz, M., Zárate, M., Zanettini, J.C., 2007b. Hoja Geológica 3569-II, San Rafael. Serv. Geol. Min. Argent. 321 (59 pp.).
Siame, L.L., Bellier, O., Sebrier, M., Araujo, M., 2005. Deformation partitioning in flat-subduction setting: case of the Andean foreland of western Argentina (28°S–33°S). Tectonics 24. http://dx.doi.org/10.1029/2005TC001787.
Sibson, R.H., 1998. Brittle failure mode plots for compressional and extensional tectonic regimes. J. Struct. Geol. 20, 655–660.
Sillitoe, R.H., 1972. A plate tectonic model for the origin of porphyry copper deposits. Econ. Geol. 67, 184–197.
Sillitoe, R.H., Hedenquist, J.W., 2003. Linkages between volcanotectonic settings, ore-fluid compositions, and epithermal precious-metal deposits. Soc. Econ. Geol. Spec. Publ. 10, 315–343.
Smith, J.V., 1996. En échelon sigmoidal vein arrays hosted by faults. J. Struct. Geol. 18, 1173–1179.
Sruoga, P., Japas, M.S., Salani, F., Kleiman, L.E., Rubinstein, N.A., 2010. Caldera La Peligrosa (47° 15′S, 71° 40′O): un evento clave en la provincia silícea Chon Aike. Rev. Asoc. Geol. Argent. 66, 368–380.
Stephens, J.R., Mair, J.L., Oliver, H.S., Hart, C.J.R., Baker, T., 2004. Structural and mechanical controls on intrusion-related deposits of the Tombstone Gold Belt, Yukon, Canada, with comparisons to other vein-hosted ore-deposit types. J. Struct. Geol. 26, 1025–1041.
Taylor, R., 2009. Ore Textures: Recognition and Interpretation. Springer-Verlag, Berlin/Heidelberg.
Tikoff, B., Greene, D., 1997. Stretching lineations in transpressional shear zones: an example from the Sierra Nevada Batholith, California. J. Struct. Geol. 19, 29–39.
Tomezzoli, R.N., Japas, M.S., 2006. Resultados paleomagnéticos preliminares en las sedimentitas neo-paleozoicas de la Formación El Imperial, Bloque de San Rafael, Mendoza. Rev. Asoc. Geol. Argent. 61, 370–382.
Tosdal, R.M., Richards, J.P., 2001. Magmatic and structural controls on the development of porphyry Cu ± Mo ± Au deposits. In: Richards, J.P., Tosdal, R.M. (Eds.), Structural Controls on Ore Deposits: Rev. Econ. Geol., 14, pp. 157–181.
von Quadt, A., Peytcheva, I., Kamenov, B., Fanger, L., Heinrich, Ch., Frank, M., 2002. The Elatsite porphyry copper deposit in the Panagyurishte ore district, Srednogorie zone, Bulgaria: U–Pb zircon geochronology and isotope–geochemical investigations of magmatism and ore genesis. In: Blundell, D.L., Neubauer, F., von Quadt, A. (Eds.), The Timing and Location of Major Ore Deposits in an Evolving Orogen: Geol. Soc. Lond. Spec. Publ., 204, pp. 119–135.
Woodcock, N.H., Fischer, M., 1986. Strike–slip duplexes. J. Struct. Geol. 8, 725–735.